

Glycolytic enzyme upregulation and numbness of mitochondrial activity characterize the early phase of apoptosis in cerebellar granule cells

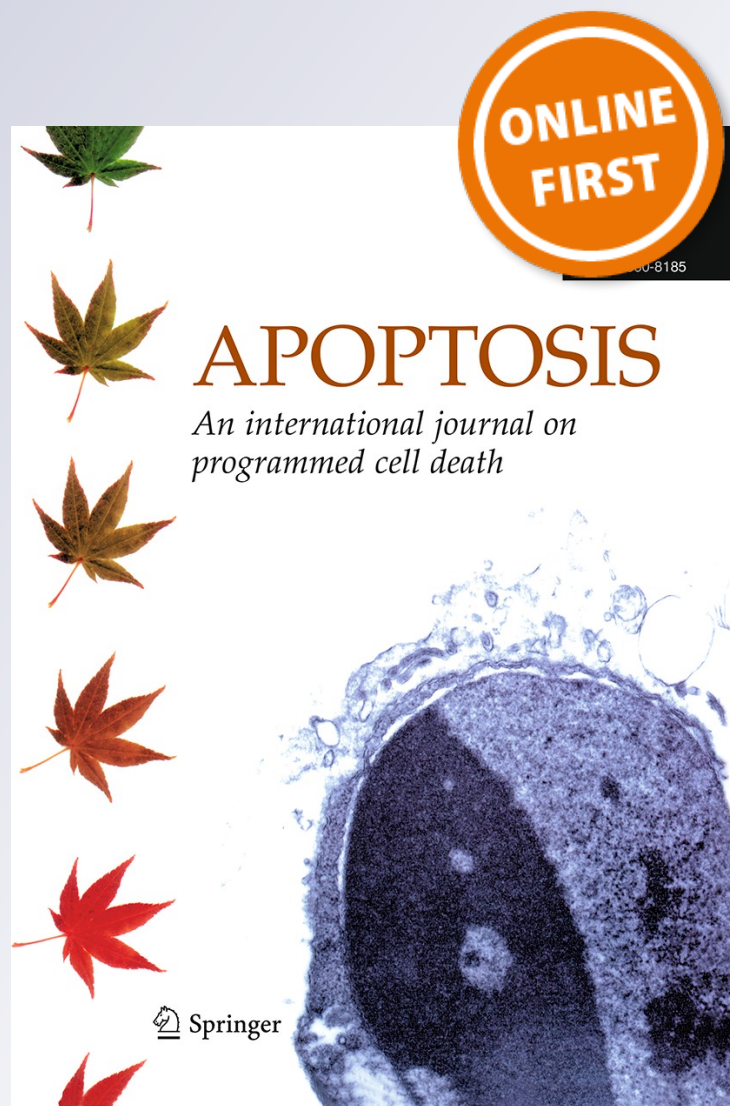
**A. Bobba, G. Amadoro, G. La Piana,
P. Calissano & A. Atlante**

Apoptosis

An International Journal on
Programmed Cell Death

ISSN 1360-8185

Apoptosis
DOI 10.1007/s10495-014-1049-1



Your article is protected by copyright and all rights are held exclusively by Springer Science +Business Media New York. This e-offprint is for personal use only and shall not be self-archived in electronic repositories. If you wish to self-archive your article, please use the accepted manuscript version for posting on your own website. You may further deposit the accepted manuscript version in any repository, provided it is only made publicly available 12 months after official publication or later and provided acknowledgement is given to the original source of publication and a link is inserted to the published article on Springer's website. The link must be accompanied by the following text: "The final publication is available at link.springer.com".

Glycolytic enzyme upregulation and numbness of mitochondrial activity characterize the early phase of apoptosis in cerebellar granule cells

A. Bobba · G. Amadoro · G. La Piana ·
P. Calissano · A. Atlante

© Springer Science+Business Media New York 2014

Abstract Alzheimer's disease (AD) and cancer proceed via one or more common molecular mechanisms: a metabolic shift from oxidative phosphorylation to glycolysis—corresponding to the activation of the *Warburg effect*—occurs in both diseases. The findings reported in this paper demonstrate that, in the early phase of apoptosis, glucose metabolism is enhanced, *i.e.* key proteins which internalize and metabolize glucose—glucose transporter, hexokinase and phosphofructokinase—are up-regulated, in concomitance with a parallel decrease in oxygen consumption by mitochondria and increase of L-lactate accumulation. Reversal of the glycolytic phenotype occurs in the presence of dichloroacetate, inhibitor of the pyruvate dehydrogenase kinase enzyme, which speeds up apoptosis of cerebellar granule cells, reawakening mitochondria and then modulating glycolytic enzymes. Loss of the adaptive advantage afforded by aerobic glycolysis, which occurs in the late phase of apoptosis, exacerbates the pathological processes underlying neurodegeneration, leading inevitably the cell

to death. In conclusion, the data propose that both aerobic, *i.e.* *Warburg effect*, essentially due to the protective numbness of mitochondria, and anaerobic glycolysis, rather due to the mitochondrial impairment, characterize the entire time frame of apoptosis, from the early to the late phase, which mimics the development of AD.

Keywords Alzheimer · Warburg · Apoptosis · Glycolytic pathway · Mitochondria · Dichloroacetate

Introduction

In the last decade, apoptosis was considered the main cause of neuronal death in some human neurodegenerative disorders, such as Alzheimer's disease (AD). More than a decade ago, Calissano's research group hypothesized a possible tight link between improper activation of apoptosis in cerebellar granule cells (CGCs) and events related to AD. CGCs survive and differentiate *in vitro* in the presence of depolarizing concentrations of KCl (25 mM) without additional need for neurotrophic factors [1]. If the serum is removed and the concentration of KCl is kept below depolarizing levels (5 mM), the majority of CGCs die by an apoptotic process [2], following a general scheme that we have extensively characterized in recent years (for a review see [3]). Briefly, in early apoptosis (0–3 h after induction) the rate of glucose oxidation by CGCs decreases [4], mitochondria are subjected to time-dependent uncoupling [4] and elevated production of reactive oxygen species (ROS) occurs [5]. Cytochrome *c* (cyt *c*) is released from the mitochondria while still coupled [5, 6] and an increase in the ATP level occurs [7]. In late apoptosis (3–8 h after induction), an alteration of the adenine nucleotide translocator (ANT-1) occurs, with ANT-1 becoming a component

A. Bobba · A. Atlante (✉)
Institute of Biomembrane and Bioenergetics (IBBE) – CNR,
Via Amendola 165/A, 70126 Bari, Italy
e-mail: a.atlante@ibbe.cnr.it

G. Amadoro
Institute of Translational Pharmacology (IFT) – CNR,
Via Fosso del Cavaliere, 100, 00133 Rome, Italy

G. La Piana
Department of Biosciences, Biotechnology and
Biopharmaceutics, University of Bari, Via Orabona, 4,
70126 Bari, Italy

P. Calissano
European Brain Research Institute (EBRI), Via del Fosso di
Fiorano, 64-65, 00143 Rome, Italy

of the mitochondrial permeability transition pore; the latter is dispensable for occurrence of apoptosis [8]. Furthermore, during the onset of CGC apoptosis, several molecular events reminiscent of AD are induced. An amyloidogenic process is activated with an increased production of A β which initiates a sort of autocrine toxic loop [9] and, contextually, Tau protein, which is the main constituent of AD neurofibrillary tangles, is cleaved by the concerted action of calpain and caspases with the production of toxic fragments [10, 11]. The mechanism of action of a Tau toxic fragment as well as of A β 1-42 has been recently elucidated and two mitochondrial proteins, *i.e.* ANT-1 and complex I, have been identified as the specific targets of such peptides, respectively [12, 13].

More recently, nerve cells selected for resistance against A β toxicity exhibit a shift in metabolism to favour L-lactate (L-LAC) production [14, 15] by expressing increased levels of pyruvate dehydrogenase kinase 1 (PDK1) accompanied by increased lactate dehydrogenase A (LDHA) activity and lactate production, when compared to control cells [14, 15]. All these changes are linked to increased glucose uptake and flux through the glycolytic pathway [16]. This switch in metabolism from mitochondrial respiration to aerobic glycolysis is a common phenotype of cancer cells and is driven in part by the hypoxia-inducible factor 1 α subunit (HIF-1 α) [17], whose activation induces transcription of glucose transporters, glycolytic enzymes, and LDHA, thereby increasing the conversion of glucose to lactate [18, 19]. Furthermore, HIF-1 suppresses mitochondrial respiration by upregulating PDK1. These findings indicate that although activation of aerobic glycolysis confers resistance to A β , cells adopting this metabolism still require a functional mitochondrial electron transport chain (ETC). The significance of this paradoxical observation is unknown but may indicate that a functional ETC is required for efficient mitochondrial oxidation of lactate and ATP production [20, 21]. Collectively, these findings indicate that PDK1- or LDHA-mediated aerobic glycolysis protects against A β toxicity while maintaining cellular ATP levels. Inefficiency of these proteins may contribute to the cognitive decline and nerve cell death observed in AD (see [15]). A recent PET imaging study, which measured both glucose consumption and oxygen utilization, revealed a strong correlation between the spatial distribution of elevated aerobic glycolysis and A β plaques in brain tissue from patients with AD, as well as from normal individuals with high levels of A β deposition but without clinical manifestation of the disease [22].

In the light of these observations, which point to the activation of an aerobic glycolytic metabolism in the surviving neurons of the AD brain [14, 15], and of our previous studies, showing that both L-LAC production and phosphofructokinase (PFK) activity increased in CGCs *en route*

to apoptosis [20, 21]—as it occurs in invasive cancer cells where this upregulation confers resistance to apoptosis [23, 24]—the aim of the present study was to evaluate in the early as well in the late phase of apoptosis: (i) the expression level and activity of glycolytic enzymes that have a key role in the metabolism of glucose, (ii) the mitochondrial activity and cell survival, either in the absence or presence of inhibitors of mitochondrial and glycolytic enzymes, as well as (iii) the glycolytic index (GI). Here we show that CGCs upregulate *Warburg effect*-enzymes in a manner reminiscent of cancer cells, in the early phase of apoptosis, thus mimicking the apoptotic resistance mechanism of surviving neurons in the AD brain. Loss of the adaptive advantage afforded by aerobic glycolysis, which occurs in the late phase, may exacerbate the pathophysiological processes associated with AD, inevitably leading neurons to death.

Materials and methods

Ethics statements

This study was performed in accordance with local ethics committee and with the principles contained in the Declaration of Helsinki as revised in 1996. All animals were handled and cared for in accordance with EEC guidelines (Directive 86/609/CEE). The animals were anesthetized and insensitive to pain throughout the procedure.

Reagents

Tissue culture medium and fetal calf serum were purchased from Gibco (Grand Island, NY, USA) and tissue culture dishes were from NUNC (Taastrup, Denmark). All enzymes and biochemicals were from Sigma Chemical Co. (St Louis, MO, USA).

Cell cultures

Primary cultures of CGCs were obtained from dissociated cerebella of 7-day-old Wistar rats as in Levi et al. [25]. Cells were plated in basal medium Eagle (BME) supplemented with 10 % fetal calf serum, 25 mM KCl, 2 mM glutamine and 100 μ g/ml gentamicin on dishes coated with poly-L-Lysine. Arabinofuranosylcytosine (10 μ M) was added to the culture medium 18–22 h after plating to prevent proliferation of non-neuronal cells.

Induction of apoptosis

Apoptosis was induced at 6–7 days *in vitro* (DIV): cells were washed and switched to a serum-free BME, containing 5 mM KCl and supplemented with 2 mM glutamine and

100 µg/ml gentamicin for the indicated times [26]. Apoptotic cells are referred to as S-K5 cells or as x-time-S-K5 to indicate the different 'x' time after apoptosis induction at which the cells are processed. In some experiments various compounds were also added simultaneously to the induction, with exposure terminated by removal of the compound-containing medium, double washing of the cell layer and replacement with fresh media. Control cells were treated identically but maintained in serum-free BME medium supplemented with 25 mM KCl for the indicated times; they are referred to as S-K25 cells. The occurrence of apoptosis was checked by measuring DNA laddering and prevention of death due to the addition of the transcriptional inhibitor actinomycin D (Act D), as in [5, 26].

CGC suspension, homogenate and cytosolic fraction preparation

The culture medium was removed and the plated CGCs were repeatedly washed with phosphate-buffered saline (PBS), containing 138 mM NaCl, 2.7 mM KCl, 8 mM Na₂HPO₄, 15 mM KH₂PO₄ pH 7.4, and then collected to obtain a *CGC suspension*. Cell integrity was quantitatively assessed by the inability of cells to oxidize externally added succinate, and by the ability of ouabain (OUA) to block glucose transport [27]. *CGC homogenate* was obtained from a cell suspension by ten strokes with a Dounce homogeniser at room temperature and appropriate checks were made to ensure the complete rupture of the plasma membrane and, at the same time, the integrity of the mitochondrial ones. The functionality of mitochondria was verified for their coupling by measuring the respiratory control index, *i.e.* (oxygen uptake rate after ADP addition)/(oxygen uptake rate before ADP addition) which reflects the ability of mitochondria to produce ATP, and for their intactness by measuring in the post-mitochondrial supernatant the activities of adenylate kinase (ADK, E.C.2.7.4.3) and glutamate dehydrogenase (GDH, E.C.1.4.1.3), essentially as in [5, 8]. *Cytosolic fractions* of both control and S-K5 CGCs (about 30×10^6 cells in 1 ml) were obtained after homogenization and centrifugation at $15,000 \times g$ for 15 min. The supernatant was indicated as cytosolic fraction. Protein content was determined, according to [28], with bovine serum albumin used as a standard.

Brain material and tissue preparation

Human brain material was provided via the rapid autopsy program of the Netherlands Brain Bank (NBB), which provides post-mortem specimens from clinically well documented and neuropathologically confirmed cases. All research involving them was conducted according to them ethical declaration of the NBB. All cases were

neuropathologically confirmed, using conventional biochemical and histopathological techniques (see [29]), and diagnosis performed using the Consortium to Establish a Registry for AD criteria. Healthy controls had no history or symptoms of neurologic or psychiatric disorders and were clinically no demented. To minimize the considerable regional differences in pathology, we selected hippocampus in all tested AD patients and relative control. The PBI-Shredder, an auxiliary high-resolution respirometry (HRR) Tool, was used to prepare homogenate—in 0.2 M phosphate buffer (pH 8.0)—of frozen tissue specimens [30], with high reproducibility of mitochondrial function as evaluated with HRR by means of Oxygraph-2 k OROBOROS®. All assays were performed on freshly homogenized tissue samples.

Assessment of neuronal viability

Viable CGCs were quantified by counting the number of intact nuclei in a haemocytometer, after lysing the cells in detergent-containing solution [31]. Cell counts were performed in triplicate and are reported as mean \pm standard deviation (SD). The data are expressed as the percentage of intact nuclei in the control cultures at each time point. Apoptosis was expressed as the percentage of intact cells with respect to control cells (%C) kept under the same respective experimental conditions. In control experiments 95–97 % integrity was found after 24 h. In some experiments, a variety of compounds were added at the induction time at the concentrations selected to avoid any possible interference with cell viability.

Polarographic measurements

O₂ consumption It was measured polarographically by means of a Gilson 5/6 oxygraph using a Clark electrode, as in [4, 8]. Cells were suspended in PBS (about 0.2 mg protein) and incubated in a thermostated (25 °C) water-jacketed glass vessel (final volume 1.5 ml). Since the incubation chamber required continuous stirring to allow O₂ to diffuse freely, the design included a magnetic stirring system which did not damage the cells in suspension. Oxygen uptake was initiated by adding glucose to the cell suspension.

Cyt c release In order to detect polarographically the cyt c presence in the extramitochondrial phase, the capability of cell homogenate to oxidise ascorbate was checked, as in ([32] and refs therein).

Glucose uptake In order to study the transport of glucose into cell, an experimental stratagem, which allows to perform the measurement under very physiological conditions,

was adopted. Briefly, glucose uptake has been followed by measuring oxygen consumption, which started by adding glucose to the cell suspension, in the absence or presence of phloretin (PHLO), a specific inhibitor of glucose transport [33]. The rate of oxygen consumption in the absence of inhibitor was lower than the one obtained as intercept at zero inhibitor concentration, showing that the inhibited step of the measured process, *i.e.* the glucose transport across the cell membrane, is not a limiting step. Thus, the activity of glucose transporter (GLUT) was obtained by calculating the reciprocal of the intercepts to the ordinate axis at the different apoptosis-times considered (for details, see “Results” section and Fig. 2B), essentially as reported in [34]. The rate of oxygen uptake was measured from the tangent to the initial part of the progress curve and expressed as $\text{natom O min}^{-1} \text{ mg}^{-1} \text{ protein}$. The sensitivity of the instrument was set so as allow rates of O_2 uptake as low as $0.5 \text{ natom min}^{-1} \text{ mg}^{-1} \text{ protein}$ to be measured.

Superoxide anion detection

$\text{O}_2^{\cdot -}$ was detected by using the MitoSox Red (for refs see [35]), a specific mitochondrial dye—highly and exclusively sensitive to superoxide, but not to other reactive oxygen/nitrogen species—which is selectively targeted to mitochondria where it accumulates as a function of mitochondrial membrane potential and exhibits fluorescence upon oxidation by superoxide and subsequent binding to mitochondrial DNA. Cell homogenate in PBS was preincubated with succinate (10 mM) plus ADP (2.5 mM) for 2 min at 25 °C. After addition of 1 μM MitoSOX Red and further 15 min incubation, fluorescence spectra ($\lambda_{\text{ex}} = 396 \text{ nm}$; λ_{em} range: 500–700 nm) were recorded using a Perkin-Elmer LS-50B Luminescence Spectrofluorimeter.

Enzyme assays

The activities of enzymes, such as hexokinase (HK) [36–38], PFK (for refs see [7, 38]), pyruvate dehydrogenase complex (PDC) [39], cytosolic L-lactate dehydrogenase (cLDH) [for refs see 21], were assayed spectrophotometrically at 340 nm ($\epsilon_{334\text{nm}} = 6.22 \text{ mM}^{-1} \text{ cm}^{-1}$), using a Jasco double-beam/double-wavelength spectrophotometer UV-550, under V_{max} conditions according to procedures briefly described below. Enzyme activities were obtained as the tangent to the initial part of the progress curves and expressed, on the basis of protein present in the specific sample, *i.e.* cell homogenate, lysate or cytosolic fraction, as nmol/min (=mU) per mg of protein, where 1 unit of enzyme activity (U) is defined as $\mu\text{mole/min}$ and the specific activity as U/mg protein. All assays, performed at least in duplicate, were at 25 °C and pH 7.2 to mimic intracellular pH.

The activity of **HK**—which catalyses the reaction $\text{ATP} + \text{glucose} \rightarrow \text{glucose-6-phosphate (G6P)} + \text{ADP}$ —was assayed through a coupled reaction with glucose-6-phosphate dehydrogenase (G6PDH), following the NADP reduction at 340 nm. The mix contained: 5 mM MgCl_2 , 8 mM ATP, 1 mM NADP, 0.1 U/ml of G6PDH and 0.5 mg cell homogenate. After 10 mM glucose addition to cell homogenate (0.5 mg protein), the activity of HK was determined by following the conversion of NADP to NADPH of the coupled reaction in which G6P is further oxidized to 6-phosphogluconate via G6PDH: $\text{G6P} + \text{NADP} + \text{H}^+ \rightarrow \text{6-phosphogluconate} + \text{NADPH} + \text{H}^+$ (for refs see [36–38]).

The activity of **PFK**—which catalyzes the phosphorylation of fructose-6-phosphate by ATP to fructose-1,6-diphosphate—was assayed in a standard coupled assay, essentially as in [7, 38]. The reaction mixture contained 5 mM KCl, 5 mM MgCl_2 , 0.2 mM NADH, 2 mM ATP, 0.4 unit/ml aldolase, 2.5 units/ml triose-phosphate isomerase, 0.4 unit/ml 3-glycerophosphate dehydrogenase and 0.5 mg cell homogenate. The reaction was initiated by adding 5 mM fructose 6-phosphate. In the assay used, fructose-1,6-diphosphate is measured by the conversion to dihydroxyacetone phosphate through the aldolase and triose phosphate isomerase reactions. The dihydroxyacetone phosphate is then reduced by the action of α -glycerophosphate dehydrogenase, oxidizing NADH to NAD.

The activity of **cLDH** was measured, as in [21], by following the absorbance changes reflecting either NADH oxidation or NAD⁺ reduction resulting from PYR or L-LAC addition, respectively, as a function of time. For the assays, cytosolic fraction (0.02 mg of protein) was incubated in the presence of NADH (0.2 mM) or NAD (1 mM) and the appropriate substrate was then added to start the reaction.

The activity of **PDC** was measured, essentially as in [39], by following NAD reduction in the presence of 10 mM KCl, 5 mM MgCl_2 , 10 mM KH_2PO_4 (pH 7.8) and 0.1 % Triton X-100 to which was added 0.5 mM NAD⁺, 200 μM Coenzyme A (CoA), 1 mM cysteine, 200 μM thiamine pyrophosphate (TPP). The presence of oxamate (OXA, 10 mM), a competitive inhibitor of the LDH, allowed the measurement of a linear rate of PDC without interference from LDH, both cytosolic and mitochondrial. The reaction was started by adding 0.4 mM pyruvate.

It was confirmed that none of the compounds used affected the enzyme activities.

Each assay was also performed at least in duplicate by using human brain postmortem specimens from clinically well documented and neuropathologically confirmed cases, which were kept frozen (–80 °C), before assays, and prepared at ice-melting temperature by homogenization of frozen tissues using the PBI-Shredder, an auxiliary HRR tool, in an assay medium consisting of Phosphate-Tris 50 mM and EDTA 2 mM pH 7.4.

Immunoblot analysis

Cell extracts for Western blot analysis were prepared by washing cells twice with PBS and lysing them in 1 % Triton X-100, 150 mM NaCl, 20 mM TrisHCl, 1 mM EGTA, 1 mM EDTA, 1 mM DTT pH 7.2, for 10 min at 4 °C in the presence of protease and phosphatase inhibitor cocktails. Lysates were immediately processed by western blot or kept frozen until assayed. Protein concentrations of the samples were estimated by the Bradford method. Equivalent amounts of proteins per sample were subjected to electrophoresis on 11 % Tricine-SDS-polyacrylamide gels [40]. The gels were then blotted onto PVDF membranes and equivalent loading of protein in each lane was assessed by brief staining of the blots with 0.1 % Ponceau Red. The following antibodies were used for analysis: anti-GLUT1, anti-GLUT2, anti-HKI, anti-HKII polyclonal antibodies (Cell Signaling Technologies, Danvers, MA, USA), monoclonal anti-PFK antibody (Chemicon) and monoclonal anti- β -actin (Sigma). HRP-conjugated secondary antibodies (Ge Healthcare, UK) were used for detection followed by enhanced chemiluminescence development (Luminata Crescendo, Millipore EMD, Darmstadt, Germany). Each membrane was stripped and re-probed with mouse anti- β -actin antibody that served as a loading control. Relative optical densities and areas of bands were quantified using a GS-700 Imaging Densitometer implemented with Molecular Analyst Software (Bio-Rad Laboratories, Hercules, CA, USA).

Measurement of L-lactate production

Cells were plated in 9-cm diameter dishes (15×10^6 cells/dish) and, after 7 DIV, apoptosis was induced, as described above. At different apoptosis times (see figure legends) aliquots of the medium were collected and the extracellular L-lactate concentrations were measured by the method of Brandt [41]; these give a reliable estimate of L-LAC production inside the cells [21, 42].

Fluorescence emission spectra of CGCs

Cell suspension (0.5 mg protein) was incubated at 25 °C in 2 ml of PBS and fluorescence emission spectra (excitation wavelength 334 nm, emission range 400–550 nm) were recorded, as in [21], using an LS50B Luminescence Spectrophotometer (Perkin-Elmer Applied Biosystems).

Determination of glycolytic activity

The cellular glycolytic activity under various experimental conditions was evaluated by measuring the GI, which was calculated by the formula: $GI = (L \times G)/O$, where L is the cellular lactate generation rate, G is glucose uptake rate, and

O is the oxygen consumption rate. To determine the cellular lactate production, cells were washed and incubated with fresh medium for the indicated times. Aliquots of the culture medium were removed for the analysis of L-LAC content as reported above. Cellular glucose uptake was measured essentially as reported above. To determine oxygen consumption, cells were suspended in PBS (about 0.2 mg protein), incubated in a thermostated (25 °C) water-jacketed glass vessel (final volume 1.5 ml) and then added with glucose. The oxygen content in the cell suspension medium was constantly monitored and oxygen consumption rate was determined as described previously [4, 8].

Statistical analysis and computing

All statistical analyses in this study were performed by SPSS software. The data were representative of at least three independent neuronal preparations (with comparable results) each one in independent measurements (in each figure legend the number of measurements is reported) and are reported as the mean with the SD. Statistical significance of the data was evaluated using the one-way analysis of variance (ANOVA) followed by post hoc Bonferroni test. $p < 0.05$ was considered as significant for all analyses.

Experimental plots were obtained using Grafit (Erithacus software); CorelDRAW graphics program was used to create the artworks.

Results

Insensitivity of apoptotic cells to mitochondrial inhibitors

Increasing amounts of mitochondrial function-affecting compounds (MFCs), including rotenone (10 ng/ml, ROT), antimycin (1 ng/ml, AA), cyanide (1 mM, CN^-), oligomycin (20 ng/ml, OLIGO) or the uncoupler carbonyl cyanide p-(trifluoromethoxy) phenylhydrazone (3 μ M, FCCP) were separately added to cultured S-K25 cells and survival was measured 24 h after drug administration. A concentration-dependent decrease in survival was observed, with 100 % death found (not shown) in all treated neurons, in good accordance with Bobba et al. [43]. Surprisingly, when MFCs, affecting either electron flow or ATP synthesis as well as mitochondrial coupling, were added to CGCs undergoing apoptosis, *i.e.* S-K5 cells, at the lowest concentration which induced 100 % death in control cells, no effect on cell survival was observed (Fig. 1A). As expected, a full recovery in survival of both S-K5 and MFC-treated S-K5 cells (not shown) was accomplished in the presence of Act D, the inhibitor of transcription which blocks apoptosis [26].

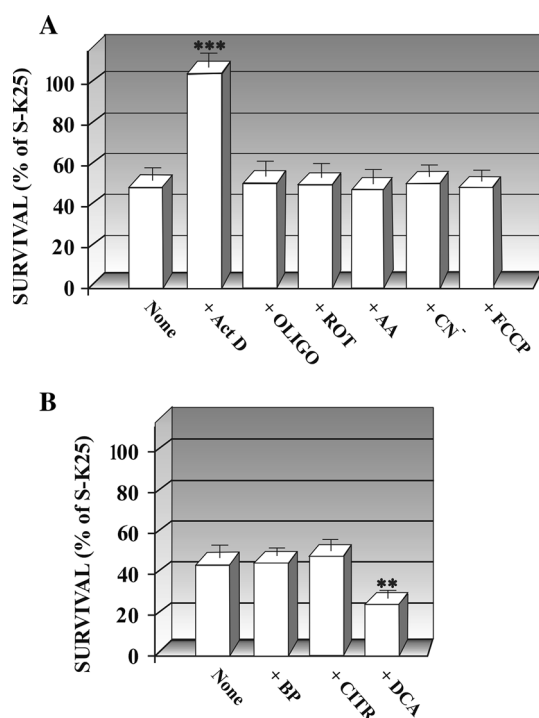


Fig. 1 Sensitivity of cell survival to various compounds in cells undergoing apoptosis. Rat CGCs (2×10^6 /well) at 7 DIV were incubated either in high potassium (S-K25) or in low potassium (S-K5) serum-free culture medium. Where indicated MFCs, *i.e.* rotenone (10 ng/ml, ROT), antimycin (1 ng/ml, AA), cyanide (1 mM, CN⁻), oligomycin (20 ng/ml, OLIGO) or the uncoupler carbonyl cyanide p-(trifluoromethoxy) phenylhydrazone (3 μ M, FCCP) (in **A**); 3-bromopyruvate (0.1 mM, BP), Citrate (CITR) or DCA (0.1 mM) (in **B**) were added separately to cultured S-K5 CGCs and survival was measured 24 h after drug administration as compared to that of control cells treated with vehicle only. Cell viability, determined by counting the number of intact nuclei, is expressed as the percentage of the S-K25 cells taken as 100 %. Control values were 100 %. Results are mean \pm SD of triplicate measurements and representative of six different experiments carried out with different cell preparations from different groups of animals. Statistical analysis was by ANOVA and Bonferroni test: ** $p < 0.01$; *** $p < 0.001$ when compared the sample with S-K5 cell (None). The lack of asterisk indicates no statistically significant differences

Glucose transporter, Hexokinase, Phosphofruktokinase and mitochondrial respiratory activities in cells undergoing apoptosis

The data of Fig. 1, *i.e.* the S-K5 cells unresponsiveness to mitochondrial inhibitors, together with the observed increase in L-LAC production and PFK activity [20, 21], beyond the fact that activities of the glycolytic enzymes are elevated [44] while some mitochondrial enzymes involved in cellular respiration [45–47] are reduced in AD brain, have led us to investigate whether glycolytic enzymes are up-regulated *en route* to apoptosis and, if so, when and how. We approached this issue essentially by using CGC homogenate as a model system. Indeed, it contains intact

and coupled mitochondria (for refs see [8]) and provides a ‘physiological’ environment for the investigation of flux of glucose through the glycolytic pathway *in situ*: this allows for simultaneously monitoring the glycolytic and mitochondrial machineries, which are closely interlinked.

First, the ability of S-K25 cells to oxidize glucose by monitoring the oxygen uptake that occurs when glucose is added to the cell suspension, according to [4], was investigated. Externally added glucose (5 mM) causes oxygen consumption ($v = 25$ natom O/min \times mg cell protein) as a result of a multistep process consisting of glucose transport across the cell membrane, entry into the glycolytic pathway, pyruvate uptake by mitochondria where oxidative decarboxylation via the PDC occurs, citric cycle and oxidative phosphorylation. The subsequent addition of cyanide (1 mM), which inhibits mitochondrial cytochrome oxidase activity, totally abolished the oxygen uptake (Fig. 2Aa), therefore showing that, besides to complete inhibition of the respiratory activity, any involvement of CN⁻-insensitive glucose oxidase activity [48] was excluded. When the measurement of oxygen consumption was carried out in the presence of PHLO (50 μ M), a competitive inhibitor of GLUT [49, 50], 3-bromopyruvate (BP, 100 μ M), a fast and powerful specific glycolytic inhibitor that affects cells by targeting HK [51, 52], or OUA (0.5 μ M), a specific inhibitor of Na⁺-K⁺ sensitive ATPase associated transport [27], a decrease of oxygen uptake (7.5, 8.6 and 11 natoms/min \times mg protein, respectively) was recorded in S-K25 cells (Fig. 2Ab), showing that glucose oxidation exclusively occurs by the glycolytic pathway and that cell membranes are intact. Interestingly, making use of an experimental strategy, it has been possible to measure the activities of GLUT, HK and mitochondrial respiratory chain (mRC) in the same experiment. Applying the control strength criterion and using each of the three specific inhibitors (see above) at different concentrations (Fig. 2B), we observed that the rate of oxygen consumption in the absence of inhibitor was lower than the value corresponding to the straight line that intercepts the Y-axis at zero inhibitor concentration—obtained by interpolating the experimental points of oxygen consumption rate in the presence of inhibitor—thus showing that the inhibited step of each measured process is not a limiting step. This was true for all the considered times of apoptosis (not shown). Then, to determine the activities of GLUT and HK in S-K5 cells taken at different times after apoptosis induction, the reciprocals of the intercept to the Y-axis were analysed and showed an increase in the activity of each enzyme which starts as soon as 30 min after apoptosis induction (Table of Fig. 2). It is worth nothing that, while GLUT activity proved to be constantly higher than that measured in S-K25 cells at all the investigated times, the increase in HK activity underwent a partial reduction at

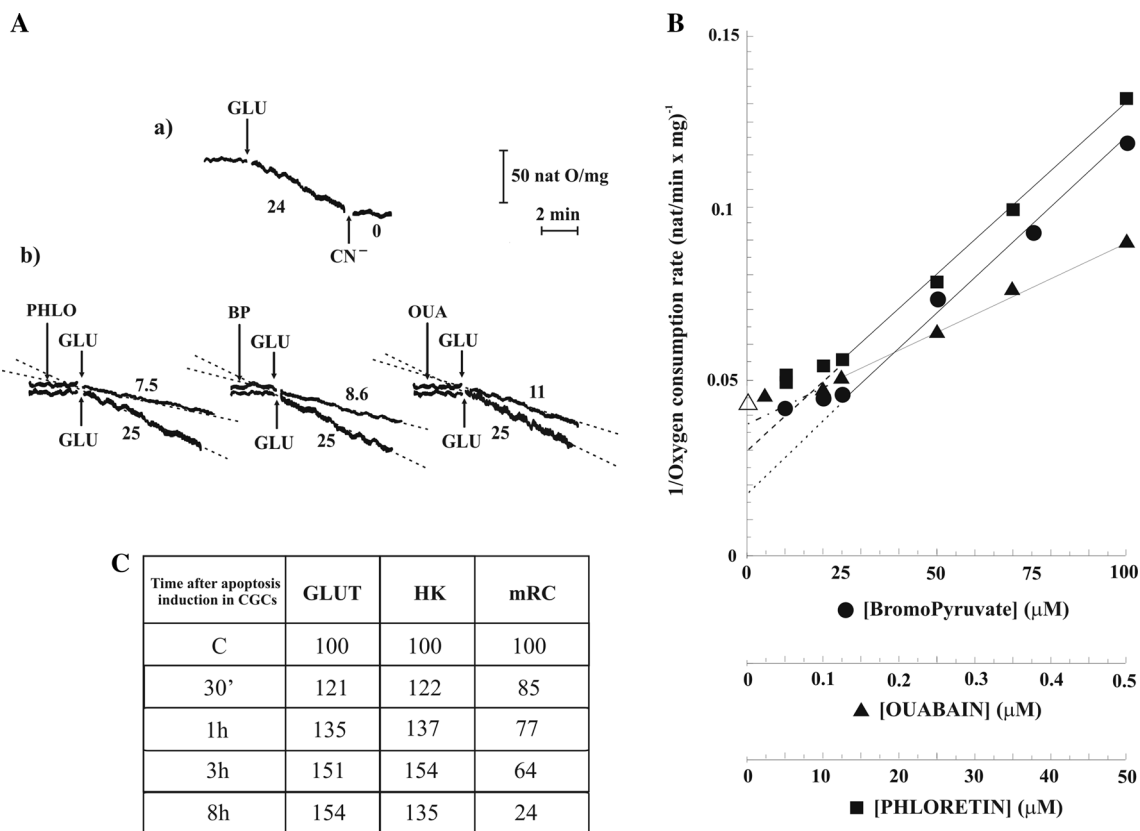


Fig. 2 Glucose oxidation: GLUT, HK and mRC activity determination. **A** S-K25 CGC suspension was incubated (0.2 mg cell protein) at 25 °C in a water-jacketed glass vessel and the consumption of O₂ was monitored polarographically. Glucose (GLU, 5 mM), CN⁻ (1 mM), PHLO (50 μM), BP (100 μM) and OUA (0.5 μM) were added to plate at the indicated times. Numbers along the curves are rates of oxygen uptake expressed as natom O/min × mg cell protein. **B** S-K25 CGC suspension was incubated (0.2 mg cell protein) at 25 °C in a water-jacketed glass vessel and the consumption of O₂ by glucose

(5 mM) was polarographically monitored either in the absence (*open triangle*) or in the presence of BP (*filled circle*), OUA (*filled triangle*) and PHLO (*filled square*) at the indicated concentrations. Reported values are the mean of three independent neuronal preparations (with comparable results) each one in triplicate with the standard deviation. **C** The activities of GLUT, HK and mRC, calculated at different times after apoptosis induction and expressed as % of control, are reported (for details see the “Results” section)

8 h, even so remaining at a value still high when compared to S-K25 cells. In the same experiment, the mitochondrial respiratory activity, *i.e.* O₂ consumption rate, was measured, in the absence of inhibitor/s, at different times after apoptosis induction in S-K5 cells, and it was proved to progressively decrease (Table of Fig. 2), consistently with [4]. On the contrary, no significant change in the glucose oxidation rate was found in CGCs of parallel cultures exposed to high [K⁺] over the same time periods (not shown).

Direct determination of both HK and PFK activities confirmed that the enzyme activities were higher in S-K5 than S-K25 cell homogenate already 30 min after apoptosis induction. The maximum enzyme activity increase in S-K5 cell homogenate (about 55 and 42 %, respectively) was measured 3 h after potassium shift, with progressive reduction up to 8 h, when the residual activity was still 25–30 % higher for both HK and PFK with respect to

control cells (Table 1a) (see Scheme 1A–C). To further confirm that our model of apoptosis represents a very valuable tool of survey, as it faithfully mimics what happens in AD, we have also performed parallel experiments in which the activities of glycolytic enzymes were measured in homogenates from autopsied brain regions of AD patients, which are endowed with Aβ accumulation and increased markers of oxidative damage [53, 54]: increased HK and PFK activities (42 and 35 %, respectively) were found (Table 1b).

In order to verify whether the increased activity of GLUT, HK and PFK was due to post-translational mechanisms or to modulation in protein expression, Western blot analyses were performed on cell homogenates by using specific antibodies. The protein levels of the two predominant GLUT isoforms found in mammalian brain, *i.e.* GLUT 1 and GLUT 3, were reported in Fig. 3A and B respectively. Consistently with results of the activity assay,

Table 1 (a) Determination of HK and PFK activities in CGCs undergoing apoptosis and (b) Determination of HK, PFK and PDC activities in Alzheimer post-mortem brains

(a)				
Time after apoptosis induction in CGCs	Enzyme activity (mU/mg cell protein)			
	Hexokinase	(%C)	Phosphofructokinase	(%C)
C	135 ± 11	100	52 ± 5	100
30'	179 ± 20	132	58 ± 4	111
1 h	196 ± 22	145	63 ± 4	121
3 h	210 ± 25	155	74 ± 5	142
8 h	171 ± 15	126	67 ± 4	129
(b)				
Enzyme activity (mU/mg postmortem specimens protein)	Age-matched controls	AD brains	<i>p</i>	(% increase)
Hexokinase	4.0 ± 0.2	5.7 ± 0.7	<0.05	42
Phosphofructokinase	0.95 ± 0.07	1.28 ± 0.14	<0.05	35
				(% decrease)
Pyruvate dehydrogenase complex	1.34 ± 0.09	0.7 ± 0.02	<0.05	48

Enzyme activity values, determined as reported in “Method” section, were the mean ± standard deviation obtained from five separate experiments carried out by using three different cell preparations (in a) or 5 and 7 different healthy cerebral samples from age-matched control and AD post-mortem cases (in b)

ANOVA and Bonferroni test: Statistically significantly differences when $p < 0.05$ (see “Materials and methods” section)

GLUT proteins showed a time-dependent increase in S-K5 cells which was significantly higher in the case of the GLUT3 isoform, reaching about 60 % increase over control at 3 h and remaining rather constant thereafter. The Western blot analysis of the HK-1 isoform (Fig. 3C) confirmed that the increased activity of this enzyme went along with a sharp increase in its protein level (59 % over control cells) as soon as 30 min after potassium shift. The same applied also to the PFK-1 protein (Fig. 3D) with about 2.0-fold increase over S-K25 cells, at 3 h after apoptosis induction.

NADH, glucose-6-phosphate and L-lactate levels in cells undergoing apoptosis

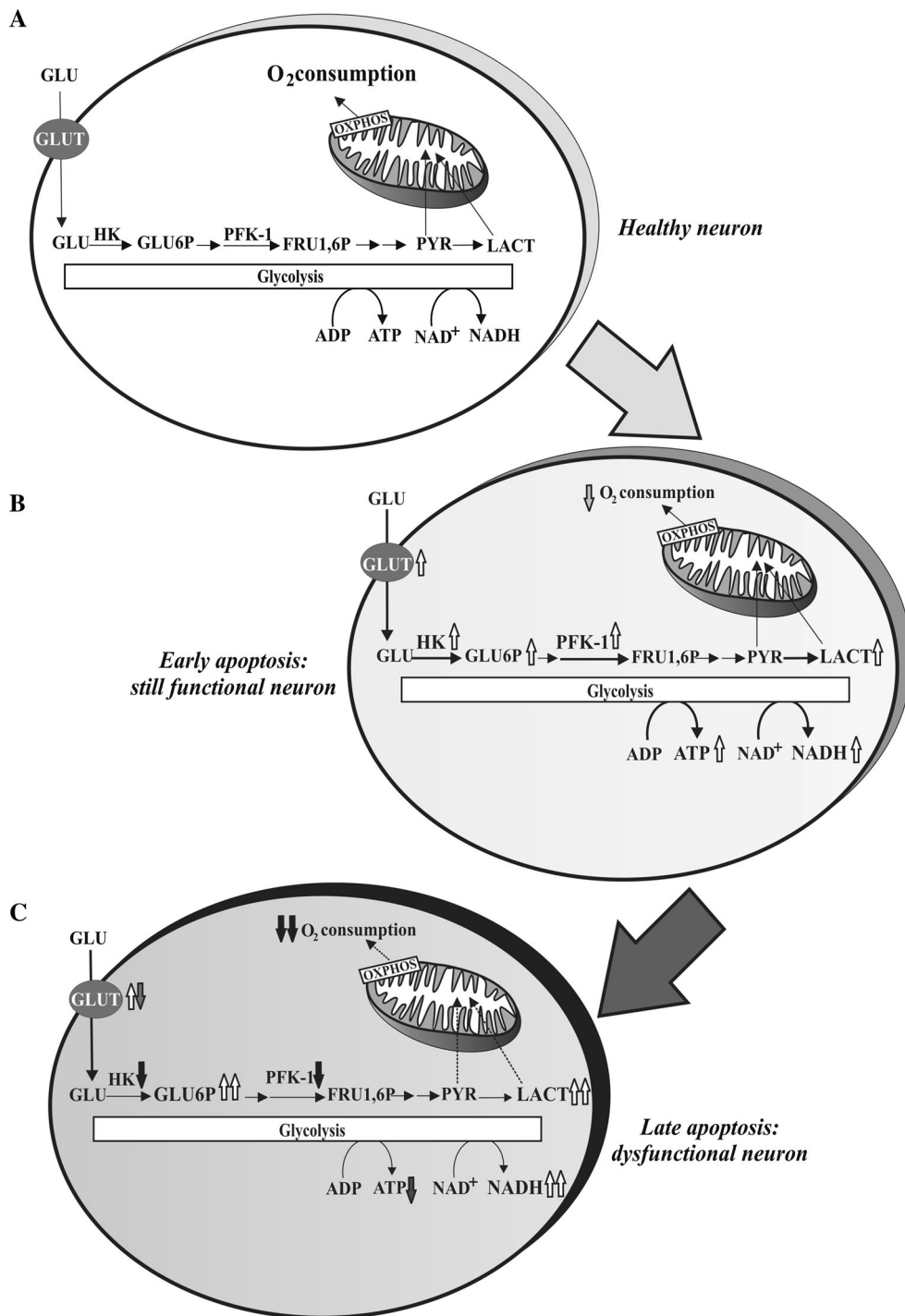
Considering that glycolysis, Krebs cycle and the respiratory chain are functionally closely coupled, any defects of mitochondrial respiration (see Fig. 1A and Table of Fig. 2A), as well as the upregulation of pathways regulating the uptake of glucose and its utilization (Figs. 2 and 3), may lead to accumulation of reduced nicotinamide adenine dinucleotide (NADH) and then to increased level of both G6P—the product in which glucose, after entry within the cell and phosphorylation, is trapped—and L-lactate, according to [21]. The inability of oxidizing cytosolic NADH was confirmed by following the cell pyridine nucleotide redox state during apoptosis. Cell emission fluorescence spectra of both control and S-K5 cells (Fig. 4A) were carried out. Fluorescence spectra of S-K5 cells showed an increase of the fluorescence

emission close to the wavelength of 456 nm, corresponding to the NADH peak, due to a time-dependent increase in intracellular NADH concentration. On the contrary, no change in the NADH fluorescence emission spectra was found in control cells. Such results are consistent with the mitochondrial activity alteration, already suggested by the results of Figs. 1 and 2.

When glucose enters the living cell, HK-catalyzed phosphorylation, which prevents any transport of glucose out from the cell, occurs. The resulting molecule G6P, besides inhibiting hexokinase in an allosterical way [55], enters into metabolic pathways, so that the uptake of glucose by cells is dependent on the rate by which G6P is metabolized. In order to substantiate the assumption that G6P level, a major biosynthetic precursor essential for synthesizing cell building blocks, increases when downstream steps are inhibited, we have measured its level in S-K5 cell homogenate (Fig. 4B), as described [56]. A gradual accumulation of G6P was observed in S-K5 cells with a percentage increase ranging from 5 to 50 % up to 8 h of apoptosis with respect to control cells (102 pmol/10⁶ S-K25 cells) (Scheme 1B).

Regarding L-LAC, we have already shown that L-LAC increases in the course of apoptosis and also that mitochondria can use the cytosolic L-LAC being endowed with specific carriers for L-LAC transport into mitochondria as well as with a LDH isoform [21]. Besides confirming the overall increase in L-LAC level (Fig. 4C), we carried out the assay of activity of cLDH in the same samples in which

Scheme 1 Time course of apoptosis: aerobic, *i.e.* Warburg effect, due essentially to the protective numbness of mitochondria, and anaerobic glycolysis, due rather to the mitochondrial impairment, characterize the entire time frame of apoptosis including the—so called—early phase, *i.e.* 0–3 h, (see **B**) and late phase, *i.e.* 3–8 h (see **C**). In **A**, the condition of healthy neuron is represented. For details see text

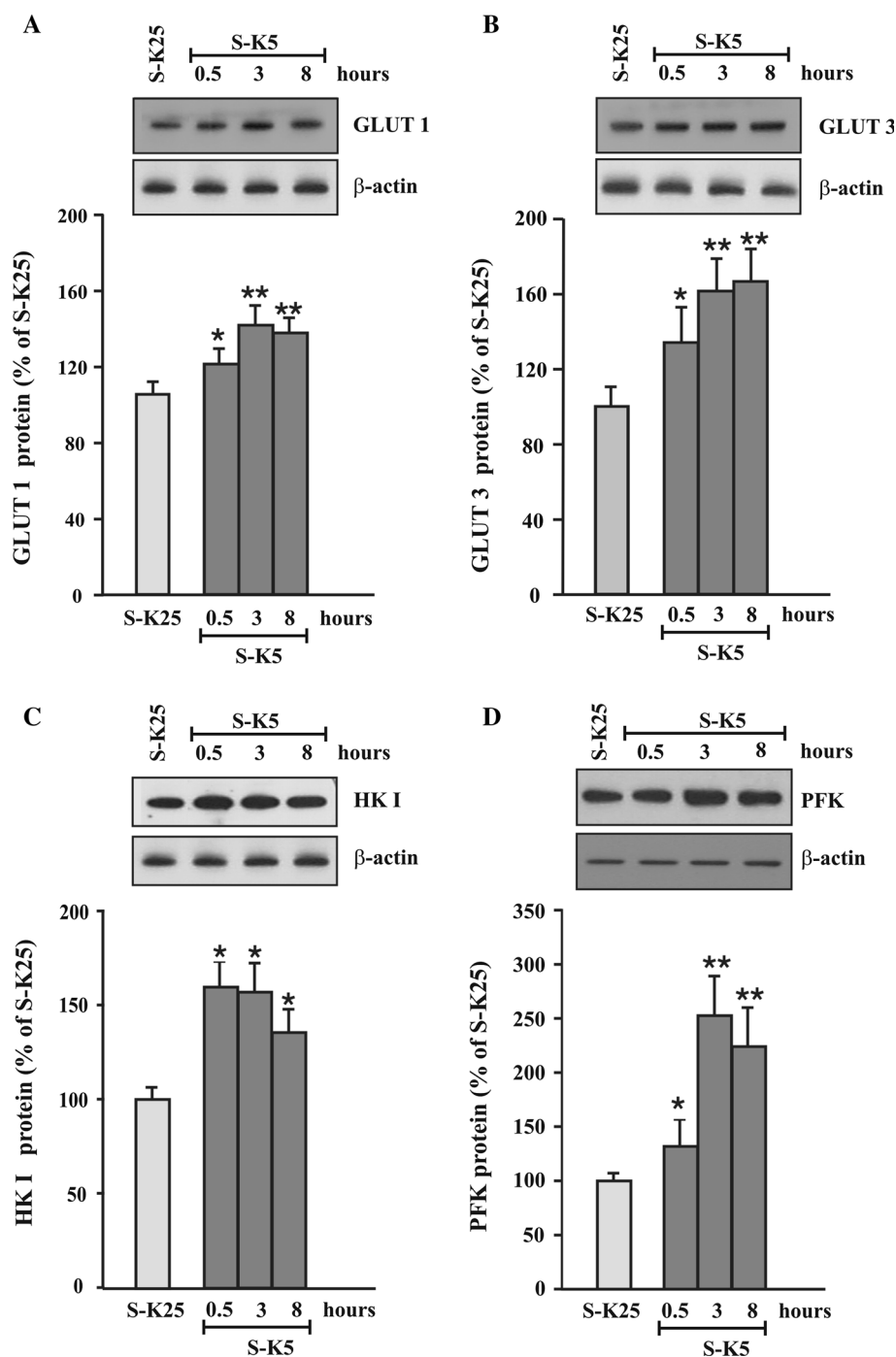


NADH and G6P were measured. Results, reported in Table 2, clearly showed an increase in V_{max} value of the reaction measured in the direction of production of L-LAC from Pyruvate. Also in this case—as for GLUT, HK and PFK—a drop in activity was found at 8 h after apoptosis induction. No difference in V_{max} of the inverse reaction, *i.e.* Lactate to pyruvate, was highlighted. Both the K_m values were unaffected.

Dichloroacetate (DCA) speeds up apoptosis of CGCs “reawakening” mitochondria and then modulating glycolytic enzymes

Having established that, in the early phase of apoptosis, glucose metabolism is enhanced, *i.e.* key enzymes which metabolize glucose are up-regulated, in concomitance with a parallel decrease in oxygen consumption by mitochondria

Fig. 3 GLUT 1, GLUT 3, HK I and PFK 1 protein expression. Cell lysates from either control (S-K25) or apoptotic CGCs (S-K5) were analyzed by Western blotting analysis with anti-GLUT 1 antibody, as described in “Materials and methods” section. Antibodies against β -actin were used to normalize the protein amount loaded onto the gel. In each panel, protein content was expressed, after normalization with respect to β -actin, as a percentage of the content in control cells to which a value of 100 was given. Values represent the mean (\pm SD) of six independent measurements with the standard deviation. ANOVA and Bonferroni test. **A** Western Blot analysis with anti-GLUT 1 antibody. * $p < 0.05$, ** $p < 0.001$; **B** Western Blot analysis with anti-GLUT 3 antibody. * $p < 0.05$, ** $p < 0.001$; **C** Western Blot analysis with anti-HK I antibody. * $p < 0.01$; **D** Western Blot analysis with anti-PFK 1 antibody. * $p < 0.05$, ** $p < 0.001$



[see 21], and taking the cue from what happens in tumor cells when *Warburg effect* is triggered (for refs see [15]), we have investigated on the activity of the mitochondrial PDC—which in the presence of oxygen, converts pyruvate into acetyl-CoA within the mitochondria [17]—in the absence or presence of DCA, a chemical inhibitor of PDK [23, 57], which regulates glucose metabolism by switching off the E1 α subunit of pyruvate dehydrogenase (PDH) [58]. In this regard, it is known that the activity of PDC is

reduced in the cerebral cortex of AD patients [23, 45–59], being likely inhibited by A β [60]. PDC activity, as measured in lysates from S-K5 cells, showed a drastic decrease (up to about 40 % at 8 h) with respect to S-K25 cells (15.2 nmol AcetylCoA produced/min x mg cell protein) (Fig. 5A). These data were corroborated by the decrease of PDC activity found in brain autoptic samples (Table 1b).

Furthermore, when DCA (100 μ M) was added to cell culture medium, the ‘presumed’ inhibition of PDK, as

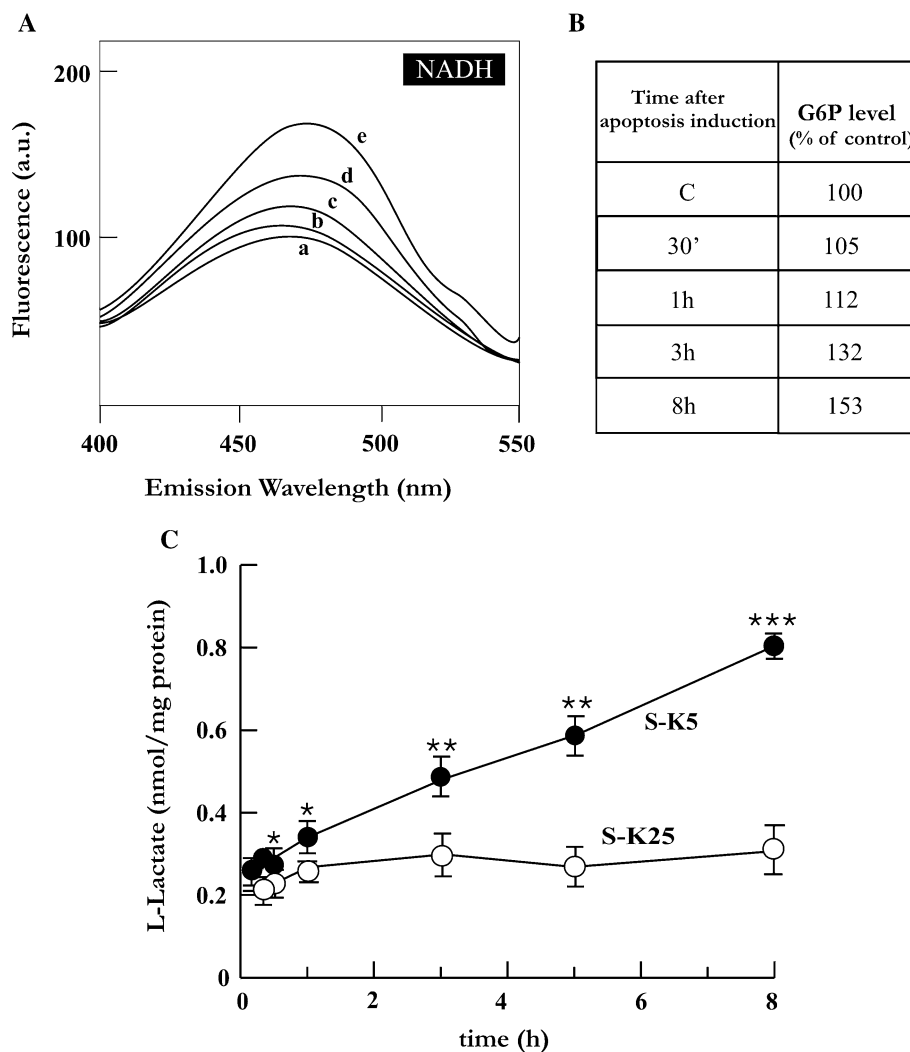


Fig. 4 NADH, Glucose-6-phosphate and L-lactate levels. **A** NADH production in CGCs undergoing apoptosis. Cell suspension was incubated at 25 °C in 2 ml PBS, with protein concentration adjusted to 0.25 mg/ml. The spectra of NADH fluorescence emission ($\lambda_{ex} = 334$ nm) of both control (a) and S-K5 cells, at different times of apoptosis, *i.e.* 30 min, 1, 3 and 8 h (b–e), were recorded as reported in “Materials and methods” section. The experiment was repeated four times with different cell preparations, giving values with 5–10 % variation. Fluorescence intensity is reported in arbitrary units (a.u.). **B** Glucose-6-phosphate production in CGCs undergoing apoptosis. The amounts of G6P was measured in cell homogenate of

S-K25 and S-K5 cells at different times of apoptosis induction. The value was expressed as % of control (S-K25) to which value 100 was given. **C** L-Lactate production in CGCs undergoing apoptosis. The amount of L-lactate was determined as a function of potassium shift time for both S-K25 (circle) and S-K5 cells (filled circle). Reported values are the mean of four independent neuronal preparations (with comparable results) each one in triplicate with the standard deviation. ANOVA and Bonferroni test: statistically significantly different with $*p < 0.05$, $**p < 0.01$, $***p < 0.001$ when comparing S-K5 with the respective S-K25 samples at the same time

described in [61], partially restores the enzymatic activity of the mitochondrial complex in S-K5 cells where a further increase up to a maximum of about 20 % was detected. On the other hand, DCA treatment was without effect on S-K25 sample.

It should be highlighted that, since the spectrophotometric assay of PDC requires appropriate cofactors as well as experimental tips based on the known properties of PDC [62], the following checks were always performed to make the enzymatic assay in good faith:

- (i) Addition of pyruvate, CoA, and NAD was obligatory for the detection of PDC activity;
- (ii) Omission of TPP led to significantly decreased enzyme activity (Fig. 5B);
- (iii) Specificity of PDC activity was confirmed by complete inhibition with the specific inhibitor 3-fluoropyruvate (FluoroPYR, 5 mM) [63] (Fig. 5B);
- (iv) That NADH oxidation was due exclusively to PDC was verified by measuring the complex

Table 2 Lactate dehydrogenase activity assay in cells undergoing apoptosis

Cytosolic LDH				
Time after apoptosis induction in CGCs	K _m ^{L-LAC} (mM)	V _{max} (μmol/min × mg protein)	K _m ^{PYR} (mM)	V _{max} (μmol/min × mg protein)
C	0.070 ± 0.006	0.57 ± 0.01	0.16 ± 0.03	36.8 ± 2.4
30'	0.046 ± 0.007	0.56 ± 0.02	0.17 ± 0.03	37.7 ± 2.6
1 h	0.053 ± 0.005	0.53 ± 0.04	0.24 ± 0.08	47.2 ± 6.7*
3 h	0.071 ± 0.002	0.59 ± 0.01	0.23 ± 0.05	78.3 ± 7.4**
8 h	0.076 ± 0.009	0.56 ± 0.02	0.21 ± 0.05	64.9 ± 5.3**

S-K25 or S-K5 cytosolic fractions (0.05 mg protein) were incubated at 25 °C in phosphate buffer 0.1 M pH 7.6 to a final volume of 1 ml. The assay was reported in the “Methods” section. The rate of absorbance increase (decrease), measured as the tangent to the initial part of the progress curve, is expressed as μmol of NADP⁺ reduced (NADPH oxidized)/min × mg of mitochondrial protein. Results are means with the standard deviation (±SD) of triplicate measurements and representative of at least 5 different experiments carried out with different cell preparations prepared from different groups of animals

ANOVA and Bonferroni test: statistically significantly different with **p* < 0.05, ***p* < 0.01, when comparing S-K5 with the respective S-K25 samples at the same time

activity in the presence of either 2-*n*-ecylquinazolin-4-yl-amine (DQA, 1 μM) [64] or OXA (10 mM) [65], inhibitors of complex I and LDH, enzymes able to oxidize NADH. Both inhibitors proved to have no effect on PDC activity (Fig. 5B).

The target of DCA inhibition, PDK, acting to maintain PDH in a catalytically active state, induces an increase in mitochondrial pyruvate consumption and then a reactivation of mitochondrial activity. In order to verify these plausible consequences, we have measured L-LAC and ROS levels by using DCA-treated S-K5 samples. As expected, the production of L-LAC in the presence of DCA significantly decreased (not shown) while the level of ROS produced by mitochondria raised (Fig. 5C), thus causing a decrease of the oxygen consumption rate due to glucose oxidation (Fig. 5D). The level of cyt *c* in the extramitochondrial phase—a ROS-depending event [5]—is also strongly increased (not shown).

Since the mRC is the major source of ROS in most cells [66], we verified whether DCA was able to induce mitochondrial production of ROS when added to culture S-K5 cells. In order to do this, a method sensitive only to superoxide of mitochondrial origin, which utilizes MitoSOX, a fluorogenic dye that selectively targets mitochondria, was adopted (see “Methods” section). In a typical experiment, emission fluorescence spectra, which exhibited a peak close to 580 nm, due to the O₂^{•-} dependent MitoSOX oxidation, were carried out (Fig. 5C) essentially as in [35]. Cell homogenate (0.2 mg protein/ml), which contains respiring mitochondria in *State 3* (*i.e.* in the presence of 10 mM succinate plus 2.5 mM ADP), was incubated with 1 μM MitoSOX with stirring at 25 °C. Mitochondrial O₂^{•-} production, measured as increase in the fluorescence emission spectra, increased in the presence of glucose,

DCA or—much more—glucose plus DCA. This effect was almost completely prevented by superoxide dismutase (SOD, 5 U/ml). No significant MitoSOX oxidation occurred when homogenate was incubated in the absence of SUC-C + ADP, nor when DCA was added to homogenate incubated with MitoSOX (not shown). As a control, it was verified that fluorescence level increased in the presence of antimycin A (AA, 0.15 μM), added after 1 min to stimulate O₂^{•-} generation by Complex III, and this effect was reversed by SOD addition (not shown). Figure 5D shows the effect of DCA on oxygen consumption caused by glucose metabolism in S-K5 cells. In a typical experiment the oxygen uptake rate, due to glucose (10 mM) oxidation, was approximately 55 natoms O/min per mg cell protein in a control sample (to which a value of 100 was given); in S-K5 cells a decrease (about 20 %) in the oxygen consumption rate was already detectable at 30 min followed by a progressive increase up to 75 % at 8 h after apoptosis induction, consistently with Fig. 2 and according to [4]. DCA (100 μM), previously added to the plate, was able to worsen the situation, causing a more severe decrease of glucose oxidation rate: at 8 h the oxygen consumption was reduced more than 90 %. No significant change was found in CGCs of sister cultures exposed to high [K⁺] over the same time periods, either in the absence or presence of DCA (not shown).

This scenario led us to examine the effect of DCA on cell viability. So, in the same experiment the responsiveness of S-K5 cells to DCA (0.1 mM), as well as to BP (0.1 mM) and citrate (10 mM), inhibitors of HK and PFK respectively, was checked at 24 h (Fig. 1B). In the presence of BP or citrate, survival was unaffected, whereas an acceleration of death was observed in the presence of DCA, which, on the contrary, was without effect on the survival of control cells, as well BP and CITR (not shown).

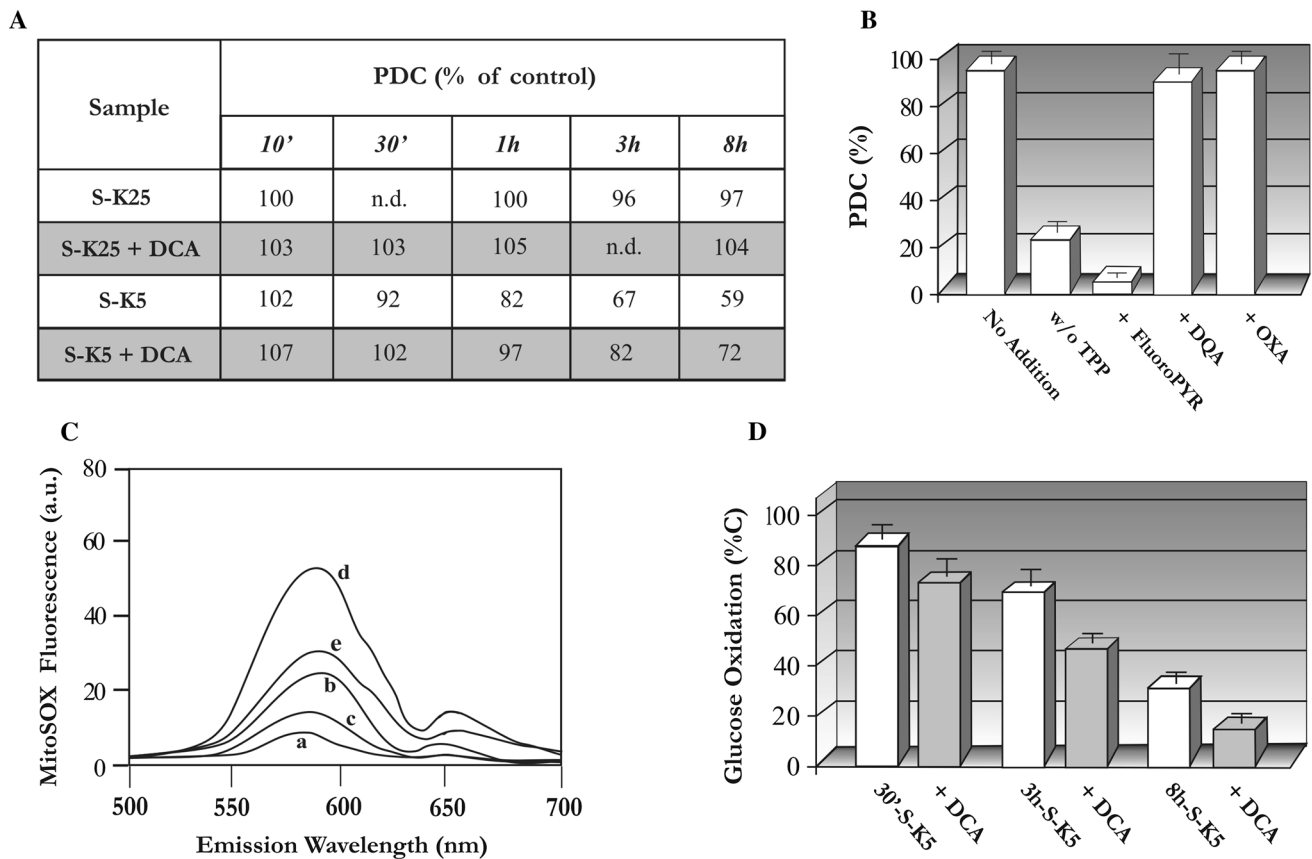


Fig. 5 DCA reawakens mitochondria and modulates glycolytic enzymes. **A** PDC enzymatic activity determination. The activity of PDC, measured in S-K25 and S-K5 cell lysates, at different times after apoptosis induction, either in the absence or presence of 0.1 mM DCA, and expressed as % of control to which value 100 is given, are reported (for details see the “Results” section). **B** Check of the validity of the PDC activity assay. Measurement of PDH activity in S-K25 lysates, expressed as % of control, were made in the absence (No Addition) or presence of 5 mM FluoroPYR, 1 μM DQA, 10 mM OXA or with the omission (w/o) of 0.2 mM TPP, are reported (for details see the “Results” section). **C** Mitochondrial ROS production. Cell homogenate (0.2 mg protein/ml), preincubated with 10 mM succinate plus 2.5 mM ADP for 2 min, was added with 1 μM MitoSOX with stirring at 25 °C. Fluorescence emission at 580 nm

was recorded after 15 min in the absence (*trace a*) or presence of 0.1 mM DCA (*trace b*), 5 mM glucose (*trace c*), glucose plus DCA (*trace d*) and in the presence of 5 units/ml SOD (*trace e*). Fluorescence spectra ($\lambda_{ex} = 396$ nm; λ_{em} range: 500–700 nm) intensity is reported in arbitrary units (a.u.). The experiment was repeated four times giving values with 5–10 % variation. **D** Glucose oxidation. CGC suspension was incubated (0.2 mg cell protein) at 25 °C in a water-jacketed glass vessel and the consumption of O₂ by 10 mM glucose was monitored polarographically in either S-K25 or S-K5 at the indicated times, in the absence or presence of 0.1 mM DCA. Reported values, expressed as % of control, are the mean of four independent neuronal preparations (with comparable results) each one in triplicate with the standard deviation

Glycolytic index gives indication of the metabolic switch between mitochondrial respiration and aerobic glycolysis in the early phase of apoptosis

The drop in oxygen consumption (Fig. 2), the increase in glucose uptake (Figs. 2 and 3) and the L-LAC accumulation (Fig. 4), observed in the early phase of apoptosis, irreducibly indicate that the glycolytic pathway is highly active in S-K5 cells. Using these three major biochemical variables, we calculated the GI, *i.e.* the proportion of glucose converted to lactate under aerobic condition, which gives indication about the metabolic switch between mitochondrial respiration and aerobic glycolysis. The GI value, obtained from the formula: $(L \times G)/O$, where L is

the cellular lactate produced, G is glucose uptake rate, and O is the oxygen consumption rate, was 0.65 in S-K25 cells over the whole time range. On the other hand, as shown in Fig. 6A, GI became 0.9 in S-K5 cells already at 10 min after apoptosis induction and increased up to 11 at 8 h. A collapse of the GI, *i.e.* the reversal of the glycolytic phenotype, in the presence of DCA was predictable: a reduction of almost 50 % at 8 h, *i.e.* $GI_{8h} = 5.8$, was observed (not shown)

In order to confirm the correlation between the GI and, for example, the % increase of NADH—with the latter (see Fig. 4) reflecting the metabolic phenotype of the cell—the correlation value was calculated. A positive and highly significant correlation was found with $R^2 = 0.95$,

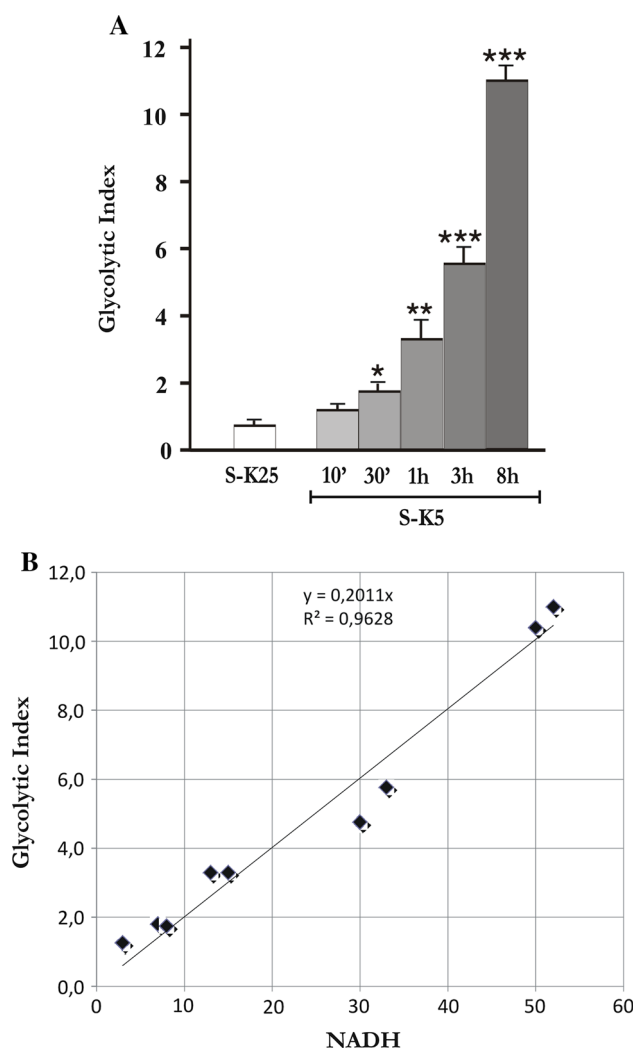


Fig. 6 **A** Glycolytic index determination and its **B** correlation with NADH level. The glycolytic index, *i.e.* the proportion of glucose converted to lactate under aerobic condition, determined by the formula: $GI = (L \times G)/O$, where L is the cellular lactate produced, G is glucose uptake rate, and O is the oxygen consumption rate, has been calculated for either S-K25 or S-K5 cells at the indicated times. Reported values are the mean of three independent neuronal preparations (with comparable results) each one in triplicate with the standard deviation. ANOVA and Bonferroni test: statistically significantly different with * $p < 0.05$, ** $p < 0.01$, *** $p < 0.001$ when comparing S-K5 with the respective S-K25 samples at the same time

indicating that the % increase of NADH level is strictly related to the increase in enzyme activities and mitochondrial impairment observed in S-K5 (Fig. 6B).

Discussion

The conventional view of central nervous system metabolism is based on the assumption that glucose is the main fuel source for active neurons and is processed in an

oxidative manner. However, since the early 1990s [21, 67], L-lactate, which was thought of as a waste metabolite, has emerged as a central player in the maintenance of neuronal function and long-term memory. Interestingly, nerve cells selected for resistance against $A\beta$ toxicity exhibit a shift in glucose metabolism to favour lactate production [14]: changes are linked to increased glucose uptake and flux through the glycolytic pathway [16]. This switch to promote aerobic glycolysis is an essential phenotype of cancer cells and is driven in part by the hypoxia-inducible factor 1α subunit (HIF- 1α) [16]. Until now, evidences suggesting that a *Warburg effect* may also exist in AD were only based upon the observation that: (i) elevated levels of HIF- 1α have been detected in two $A\beta$ -resistant-nerve like cell lines, *i.e.* PC12 and B12 [14], as well as in the brains of AD transgenic mice as compared to controls [14]; and (ii) HIF- 1α stimulates expression of GLUTs and glycolytic enzymes in $A\beta$ -resistant cells [16], thereby increasing the conversion of glucose to pyruvate, and induces the transcription of LDHA, resulting in an increase in the lactate production when compared to control cells [14]. As a result, mitochondrial-derived ROS, which are closely associated with $A\beta$ toxicity [13], are markedly diminished in resistant-with respect to sensitive-cells [14]. Consistently, the reduction of various mitochondrial enzymes involved in cellular respiration has been observed in AD brain [45–47] and measurements of ATP showed that its synthesis by OXPHOS is decreased in 7WD4 and 7PA2 cells by $\sim 25\%$, with this loss being partly compensated by glycolysis [68].

Understanding how nerve cells become resistant to $A\beta$ toxicity is the focal point for understanding how some nerve cells, within the AD brain, are able to survive while large number of cells die. In parallel, the question arises as to why decreased mitochondrial respiration in $A\beta$ -resistant cells would be advantageous [14]. In order to give an adequate explanation to this question, we have chosen to use CGCs as experimental model because, during the onset of apoptosis, several molecular events reminiscent of AD, such as activation of the amyloidogenic process, cleavage of tau and production of toxic fragments, are induced (see [69] and refs therein). The starting point that prompted us to perform this study has been the observation that mitochondrial inhibitors, *i.e.* OXPHOS inhibitors, administered at the time of apoptosis induction—while killed control cells [43]—had no effect on S-K5 cell survival (Fig. 1A), just as though mitochondria of these cells were anesthetized.

The strength of this paper relies on some strategic experimental conditions used to measure the activities, as well as the protein levels, of the glycolytic enzymes, both cytosolic and mitochondrial, at different times during the apoptosis progression, *i.e.* in the early and late phases which correspond to the mild and severe AD stages (see

Scheme 1A–C) respectively. The results, herein reported, shed light and clarify, once for all, whether a bioenergetic mechanism may be the keystone responsible for the metabolic dysregulation which associates cancer and AD. That the cells, subjected to an apoptotic stimulus, activate a *Warburg effect*-like mechanism, *i.e.* suppression of OXPHOS combined with activation of aerobic glycolysis as the main pathway for ATP synthesis [70, 71], is suggested by the results of Figs. 2, 3, 4 and 6, in which an up-regulation of GLUT, HK, PFK and cLDH together with an increase of GI value are observed, and of Fig. 5, where a reduced PDC activity, partially restored by DCA, is reported.

These points will be discussed separately.

Glucose transporter

Regardless of the ultimate fate of glucose within brain, the initial step in glucose metabolism is the passage across the cell membrane. Glucose, in fact, is transported into cells by facilitative transporters and then trapped intracellularly by phosphorylation [72]. Thus, the first objective of this paper has been to study the glucose transport: as described in Fig. 2, an increase in activity of GLUT was detected in the early phase of apoptosis, which is accompanied by an upregulation of GLUT1 and, even more, GLUT 3 protein levels (Fig. 3), the two isoforms mainly expressed in the brain (reviewed in [73]). In the late phase of apoptosis a plateau is reached with no further increase in both activity and protein levels. In this regard, the doubt that the reduced glucose uptake was due to neuronal loss was eluded by *in vitro* studies suggesting that A β inhibition of neuronal glucose uptake precedes neuronal degeneration [74, 75], as well by the evidence that low cerebral glucose uptake in individuals genetically at risk for developing AD was observed [76–78].

Hexokinase and phosphofructokinase

An increase, followed by a drastic collapse of the activities as well as, although to a less extent, of the protein levels depending on the progression of apoptosis, was found in the case of HK and PFK (Fig. 2; Table 1), the more important glycolytic enzymes which play a critical role in ATP production. As in the early phase of apoptosis, increased activities of enzymes involved in glycolysis have also been observed in malignant cells and tissues [79–81] and, furthermore, they are higher in metastases than in primary tumors, suggesting an association between glycolysis and tumor progression [82]. More puzzling are the data on HK: its decreased activity has been reported in brain, fibroblasts, leukocytes and microvessels of patients with AD (for refs see [44]); Mortilla and Sorbi [83] found no differences in its activity between AD and control

patients while Iwangoff et al. [84] observed an increased activity of the enzyme, consistent with our results (see Table 1). All to say that results are not just remarkably bizarre and controversial but, as stressed by Bigl et al. [85], have to be considered with caution because the experimental conditions for the preparation of cell-free extracts and activity determination may not be optimal and may lead to instability of enzymes after tissue disintegration.

The same applies to PFK: although in several studies the activity of PFK has been found to be strongly diminished in postmortem AD brains (for refs see [44]), contrarily to our results (see Table 1), but consistently with Bigl et al. [85] who reported up to a 90 % reduction of PFK activity in frontal and temporal cortex of AD patients, and Pla et al. [86] who found a decrease in the rat brain PFK activity during a period of 24 h after death preceded by an early increase after 1 h, in certain areas of the brain of AD patients the increased activity of PFK was found to be associated with an increased steady state mRNA level of PFK. The increased expression of the gene of a key glycolytic enzyme does not simply fit with the decreased cerebral metabolism in AD (reviewed in [87]), but, as recently stated by several authors, could suggest that the pathophysiology in AD may be more complex than previously thought.

Anyway it should be noted that unlike from the results of the enzymatic activity assays, which tend to decrease after 8 h when compared to the values reached at 3 h (see Scheme 1C), the levels of HK and PFK proteins do not decrease significantly with the progression of apoptosis (Fig. 3), leaving assume that a regulatory mechanism, beyond the level of the two proteins, could be responsible for the final modulation of the enzyme activities.

Mitochondrial function and glycolytic index

That the CGCs in the early phase of apoptosis, like several cancer cells [88], mainly use glycolysis—as evinced by the upregulation of glycolytic enzymes (see above) (Scheme 1 compare a with b)—is suggested also by the ‘apparent’ numbness of mitochondria, mentioned above. The impairment of mitochondrial metabolism in AD has already been well documented (for refs see [15]), but this is the first time that the mitochondrial quiescence is experimentally declared. Regarding this, it has been shown that the mitochondrial inhibitors failed to kill cells depleted of mitochondrial DNA and, hence, lacking an intact respiratory chain (for refs see [71]), suggesting that mitochondria are sent into quiescence in the early phase of apoptosis in the fruitless attempt of cells to oppose the forthcoming death.

However, although activation of aerobic glycolysis renders mitochondria unresponsiveness to inhibitors, cells which adopt this metabolism still require a functional

mitochondrial ETC both for A β to elicit a toxic effect [13, 14] and for efficient mitochondrial oxidation of L-LAC [21] whose level rises (Fig. 4), along with that of G6P and of the NADH/NAD⁺ ratio (Fig. 4), as is fitting. The increase in G6P deserves a deep discussion which, however, need to be postponed (*manuscript in preparation*). It is widely known, in fact, that the association between HK and the Voltage-dependent anion channel (VDAC), as well the high cellular concentrations of the reaction product G6P, causes a conformational change of the HK enzyme, resulting in its detachment from VDAC and modulation of its activity. This scenario, greatly affecting the progression of apoptosis, has prompted us to investigate the molecular mechanism responsible for the entire process in a dedicated study.

That aerobic glycolysis is the cause of L-LAC accumulation in cancer cells, due to the elevated levels of cLDH, converting pyruvate to lactate (for refs see [89]), has been also proved in our model (Table 2). In contrast no effect on mitochondrial LDH was found in S-K5 cells [21].

The calculation of GI value for the S-K5 cells has shown that it already increases 10 min after apoptosis induction, with a decisive jump at 3 h, a time at which the peak of increased activity of the tested glycolytic enzymes is found. The GI further increases 8 h after apoptosis starts, *i.e.* in the late phase, when the protective glycolytic phenotype is already lost. Similar biochemical alterations, indicative of highly increased glycolysis, were also observed in the ρ^- cell clones derived from Raji cells [90]. It is worthy to be noted that, considering our previous results on the ATP level and its synthesis [7, 8], when the OXPHOS was completely blocked by OLIGO, a decrease in the ATP content was found, but nonetheless cells still died by apoptosis. In this case, ATP was provided by anaerobic glycolysis, as suggested by the large increase of L-LAC production [7]. Therefore we would dare to propose, in the light of old and new results, that both aerobic, *i.e.* Warburg effect, due essentially to the protective numbness of mitochondria, and anaerobic glycolysis, due rather to the mitochondrial impairment, characterize the entire time frame of apoptosis including the—so called—early phase, *i.e.* 0–3 h, (see Scheme 1B) and late phase, *i.e.* 3–8 h (see Scheme 1C).

Consistent with this hypothesis, the inhibition of PDK, *i.e.* activation of PDH (Table of Fig. 5), using the chemical inhibitor DCA, was shown to reverse the glycolytic phenotype—which characterizes the early phase in our model of apoptosis—lowering lactate level and raising, as expected, mitochondrial ROS (Fig. 5C) production, which is associated with the enhanced consumption of oxygen in the OXPHOS reaction—ironically, the awakening of mitochondria is responsible for an acceleration of their impairment, *i.e.* like a dog chasing its tail—which is

ultimately responsible for the speeding up of the death (Fig. 1b), without any effect on control cells. The DCA-dependent Warburg effect reversal, as already documented in a number of cancer cell lines [91], has been also substantiated by the GI value which is lowered by approximately 50 % in the presence of DCA. DCA data suggest that the glycolytic phenotype of cell undergoing apoptosis—in the early phase of the cascade events—plays a protective role towards mitochondria, just falling asleep them.

This picture, which sees the concerted involvement of activated glycolytic enzymes, depression of the mitochondrial function and consequently accumulation of L-LAC, NADH and G6P, reflects the metabolic condition of A β -resistant cells. Recent neuroimaging studies have shown that the spatial distribution of aerobic glycolysis in the brains of AD patients strongly correlates with A β deposition. Interestingly, clonal nerve cell lines selected for resistance to A β exhibit increased glycolysis as a result of activation of the transcription factor HIF1, in a manner reminiscent of cancer cells [92]. In particular, A β -resistant nerve cell lines showed elevated PDK1 expression in addition to an increase in LDH activity and lactate production when compared to control cells. In addition, mitochondrial derived ROS were markedly diminished in A β -resistant but not in sensitive cells, thus suggesting that a change in ROS metabolism is a key component of A β toxicity as well as an element responsible for the phenotype of the A β -resistant cells [13, 93].

In this regard, we need to point out that the measurement of biochemical activities in AD brain is a measurement only restricted to viable A β -resistant cells (see [93]), and not to dying cells as is frequently assumed. Based upon the observations collected with A β -resistant cell lines, it would be predicted that AD brain would have elevated glycolytic activities, consistently with [16], as also confirmed in our assays on post-mortem samples (Table 1). On the other hand, there have been claims that some glycolytic enzyme activities are decreased in AD brain (see, for example, [94]), but these contradictory data could be due to a delayed time to autopsy or different cryopreservation techniques.

Now, although the Warburg-phenotype may contribute to the implementation of apoptotic resistance mechanisms in surviving neurons of the AD brain, only some cells resist, so as to oppose the neurodestructive wave, *i.e.* the irreversible late phase. Consistently, Minervini et al. [95] found that glutamate caused cytotoxicity in embryonic CGs although there was an increase in glucose uptake, suggesting that the increase was insufficient to ensure the survival.

The scenario which comes out from the research in object suggests that the development of AD and of many

cancers may proceed via one or more common molecular mechanisms: a metabolic shift from OXPHOS to glycolysis occurs in both diseases. This means that a shift from OXPHOS to glycolysis in AD neurons would only be a transient attempt to rescue neurons; contrariwise, cancer cells shut down OXPHOS and mitochondria-mediated apoptotic signalling, making themselves resistant to apoptotic cell death and independent from mitochondrial ATP production. The activities of glycolytic enzymes are increased in cancer cells, and the ATP produced is sufficient for cell survival. In both types of diseases, the mitochondrial function is impaired: the difference is that cancer cells evolve to survive without OXPHOS while neurons can neither function properly nor survive without OXPHOS, with the exception of those cells that, by virtue of 'majeure force', safeguard the Warburg phenotype, contributing to resistance against A β toxicity and becoming A β -resistant cells. Understanding how nerve cells become resistant to A β toxicity will be central to understanding how some nerve cells, within the AD brain, are able to survive while the majority die. However, although the physiological relevance of these findings in an in vivo AD model remains unknown, the characterization of the mechanisms by which glycolysis is upregulated in A β resistant cells could reveal possible targets for drug therapy in the treatment of AD.

Acknowledgments The authors thank the native English-speaker for linguistic consultation and Messrs Vito A. Petragallo and Riccardo S. Merafina for their skilful technical assistance. This research was supported by: Project FIRB-MERIT—RBNE08HWLZ_012 to M.N.G. and PRIN 2010-2011 (prot. 2010 M2JARJ-003) to G.A.

References

- Gallo V, Ciotti MT, Aloisi F, Levi G (1986) Developmental features of rat cerebellar neural cells cultured in a chemically defined medium. *J Neurosci Res* 15:289–301
- Galli C, Meucci O, Scorziello A, Werge TM, Calissano P, Schettini G (1995) Apoptosis in cerebellar granule cells is blocked by high KCl, forskolin, and IGF-1 through distinct mechanisms of action: the involvement of intracellular calcium and RNA synthesis. *J Neurosci* 15:1172–1179
- Bobba A, Atlante A, de Bari L, Passarella S, Marra E (2004) Apoptosis and cytochrome *c* release in cerebellar granule cells. *In Vivo* 18:335–344
- Atlante A, Gagliardi S, Marra E, Calissano P (1998) Neuronal apoptosis in rats is accompanied by rapid impairment of cellular respiration and is prevented by scavengers of reactive oxygen species. *Neurosci Lett* 245:127–130
- Atlante A, Bobba A, Calissano P, Passarella S, Marra E (2003) The apoptosis/necrosis transition in cerebellar granule cells depends on the mutual relationship of the antioxidant and the proteolytic systems which regulate ROS production and cytochrome *c* release *en route* to death. *J Neurochem* 84:960–971
- Bobba A, Atlante A, Giannattasio S, Sgaramella G, Calissano P, Marra E (1999) Early release and subsequent caspase-mediated degradation of cytochrome *c* in apoptotic cerebellar granule cells. *FEBS Lett* 457:126–130
- Atlante A, Giannattasio S, Bobba A, Gagliardi S, Petragallo V, Calissano P, Marra E, Passarella S (2005) An increase in the ATP levels occurs in cerebellar granule cells en route to apoptosis in which ATP derives from both oxidative phosphorylation and anaerobic glycolysis. *Biochim Biophys Acta* 1708:50–62
- Atlante A, Bobba A, de Bari L, Fontana F, Calissano P, Marra E, Passarella S (2006) Caspase-dependent alteration of the ADP/ATP translocator triggers the mitochondrial permeability transition which is not required for the low-potassium dependent apoptosis of cerebellar granule cells. *J Neurochem* 97:1166–1181
- Galli C, Piccini A, Ciotti MT, Castellani L, Calissano P, Zaccheo D, Tabaton M (1998) Increased amyloidogenic secretion in cerebellar granule cells undergoing apoptosis. *Proc Natl Acad Sci USA* 95:1247–1252
- Canu N, Dus L, Barbato C, Ciotti MT, Brancolini C, Rinaldi AM, Novak M, Cattaneo A, Bradbury A, Calissano P (1998) Tau cleavage and dephosphorylation in cerebellar granule neurons undergoing apoptosis. *J Neurosci* 18:7061–7074
- Amadoro G, Serafino AL, Barbato C, Ciotti MT, Sacco A, Calissano P, Canu N (2004) Role of N-terminal tau domain integrity on the survival of cerebellar granule neurons. *Cell Death Diff* 11:217–230
- Atlante A, Amadoro G, Bobba A, de Bari L, Corsetti V, Pappalardo G, Marra E, Calissano P, Passarella S (2008) A peptide containing residues 26–44 of tau protein impairs mitochondrial oxidative phosphorylation acting at the level of the adenine nucleotide translocator. *Biochim Biophys Acta* 1777:1289–1300
- Bobba A, Amadoro G, Valenti D, Corsetti V, Lassandro R, Atlante A (2013) Mitochondrial respiratory chain Complexes I and IV are impaired by β -amyloid via direct interaction and through Complex I-dependent ROS production, respectively. *Mitochondrion* 13:298–311
- Newington JT, Pitts A, Chien A, Arseneault R, Schubert D, Cumming RC (2011) Amyloid beta resistance in nerve cell lines is mediated by the Warburg effect. *PLoS One* 6:ID e19191
- Newington JT, Harris RA, Cumming RC (2013) Reevaluating metabolism in Alzheimer's disease from the perspective of the astrocyte-neuron lactate shuttle model. *J Neurodegener Dis*. doi:10.1155/2013/234572
- Soucek T, Cumming R, Dargusch R, Maher P, Schubert D (2003) The regulation of glucose metabolism by HIF-1 mediates a neuroprotective response to amyloid β peptide. *Neuron* 39:43–56
- Papandreou I, Cairns RA, Fontana L, Lim AL, Denko NC (2006) HIF-1 mediates adaptation to hypoxia by actively downregulating mitochondrial oxygen consumption. *Cell Metab* 3:187–197
- Semenza GL (1996) Transcriptional regulation by hypoxia-inducible factor 1: molecular mechanisms of oxygen homeostasis. *Trends Cardiovasc Med* 6:151–157
- Semenza GL, Jiang BH, Leung SW, Passantino R, Concordet JP, Maire P, Giallongo A (1996) Hypoxia response elements in the aldolase A, enolase 1, and lactate dehydrogenase A gene promoters contain essential binding sites for hypoxia-inducible factor 1. *J Biol Chem* 271:32529–32537
- Passarella S, de Bari L, Valenti D, Pizzuto R, Paventi G, Atlante A (2008) Mitochondria and L-lactate metabolism. *FEBS Lett* 582:3569–3576
- Atlante A, de Bari L, Bobba A, Marra E, Passarella S (2007) Transport and metabolism of L-lactate occur in mitochondria from cerebellar granule cells and are modified in cells undergoing low potassium dependent apoptosis. *Biochim Biophys Acta* 1767:1285–1299
- Vlaskin AG, Vaishnavi SN, Couture L, Sacco D, Shannon BJ, Mach RH, Morris JC, Raichle ME, Mintun MA (2010) Spatial correlation between brain aerobic glycolysis and amyloid- β (A β) deposition. *Proc Natl Acad Sci USA* 107:17763–17767
- Bonnet S, Archer SL, Allalunis-Turner J, Haromy A, Beaulieu C, Thompson R, Lee CT, Lopaschuk GD, Puttagunta L, Bonnet S,

- Harry G, Hashimoto K, Porter CJ, Andrade MA, Thebaud B, Michelakis ED (2007) A mitochondria-K⁺ channel axis is suppressed in cancer and its normalization promotes apoptosis and inhibits cancer growth. *Cancer Cell* 11:37–51
24. Michelakis ED, Webster L, Mackey JR (2008) Dichloroacetate (DCA) as a potential metabolic-targeting therapy for cancer. *Br J Cancer* 99:989–994
25. Levi G, Aloisi F, Ciotti MT, Gallo V (1984) Autoradiographic localization and depolarization-induced release of acidic amino acids in differentiating cerebellar granule cell cultures. *Brain Res* 290:77–86
26. D'Mello SR, Galli C, Ciotti MT, Calissano P (1993) Induction of apoptosis in cerebellar granule neurons by low potassium: inhibition of death by insulin-like growth factor I and cAMP. *Proc Natl Acad Sci USA* 90:10989–10993
27. Sjodin RA (1989) Measurement of Na⁺-K⁺ pump in muscle. *Methods Enzymol* 173:695–714
28. Waddell WJ, Hill C (1956) A simple ultraviolet spectrophotometric method for the determination of protein. *J Lab Clin Med* 48:311–314
29. Amadoro G, Corsetti V, Atlante A, Florenzano F, Capsoni S, Bussani R, Mercanti D, Calissano P (2012) Interaction between NH₂-tau fragment and A β in Alzheimer's disease mitochondria contributes to the synaptic deterioration. *Neurobiol Aging* 33: 833.e1–833.e25
30. Draxl A, Eigentler A, Gnaiger E (2013) PBI-Shredder HRR-Set: preparation of tissue homogenates for diagnosis of mitochondrial respiratory function. *Mitochondrial Physiol Netw* 17(02):1–8
31. Volontè C, Ciotti MT, Battistini L (1994) Development of a method for measuring cell number: application to CNS primary neuronal cultures. *Cytometry* 17:274–276
32. Atlante A, Bobba A, Paventi G, Pizzuto R, Passarella S (2010) Genistein and daidzein prevent low potassium-dependent apoptosis of cerebellar granule cells. *Biochem Pharmacol* 79:758–767
33. Yokota K, Nishi Y, Takesue Y (1983) Effect of phloretin on Na⁺-dependent D-glucose uptake by intestinal brush border membrane vesicles. *Biochem Pharmacol* 32:3453–3457
34. Atlante A, Passarella S, Minervini GM, Quagliariello E (1994) Glutamine transport in normal and acidotic rat kidney mitochondria. *Arch Biochem Biophys* 315:369–381
35. Bobba A, Amadoro G, Petragallo VA, Calissano P, Atlante A (2013) Dissecting the molecular mechanism by which NH₂tau and A β 1-42 peptides impair mitochondrial ANT-1 in Alzheimer disease. *Biochim Biophys Acta* 1827:848–860
36. MacDonald MJ (1989) Does glyceraldehyde enter pancreatic islet metabolism via both the triokinase and the glyceraldehyde phosphate dehydrogenase reactions? A study of these enzymes in islets. *Arch Biochem Biophys* 270:15–22
37. Ahmad A, Ahmad S, Schneider BK, Allen CB, Chang LY, White CW (2002) Elevated expression of hexokinase II protects human lung epithelial-like A549 cells against oxidative injury. *Am J Physiol Lung Cell Mol Physiol* 283:L573–L584
38. Lubec B, Chiappe-Gutierrez M, Hoeger H, Kitzmueller E, Lubec G (2000) Glucose transporters, hexokinase, and phosphofructokinase in brain of rats with perinatal asphyxia. *Pediatric Res* 47:84–88
39. Chretien D, Pourrier M, Bourgeron T, Séné M, Rötig A, Munnich A, Rustin P (1995) An improved spectrophotometric assay of pyruvate dehydrogenase in lactate dehydrogenase contaminated mitochondrial preparations from human skeletal muscle. *Clin Chim Acta* 240:129–136
40. Schägger H (2006) Tricine-SDS-PAGE. *Nat Protoc* 1:16–22
41. Brandt RB (1982) Determination of D-lactate in plasma. *Methods Enzymol* 89:35–40
42. Walz W, Mukerji S (1988) Lactate release from cultured astrocytes and neurons: a comparison. *Glia* 1:366–370
43. Bobba A, Atlante A, Azzariti A, Sgaramella G, Calissano P, Marra E (2004) Mitochondrial impairment induces excitotoxic death in cerebellar granule cells. *Int J Mol Med* 13:873–876
44. Bigl M, Bruckner MK, Arendt T, Bigl V, Eschrich K (1999) Activities of key glycolytic enzymes in the brains of patients with Alzheimer's disease. *J Neural Transm* 106:499–511
45. Gibson GE, Sheu KF, Blass JP (1998) Abnormalities of mitochondrial enzymes in Alzheimer disease. *J Neural Transm* 105:855–870
46. Brooks WM, Lynch PJ, Ingle CC, Hatton A, Emson PC, Faull RL, Starkey MP (2007) Gene expression profiles of metabolic enzyme transcripts in Alzheimer's disease. *Brain Res* 1127:127–135
47. Liang WS, Reiman EM, Valla J, Dunckley T, Beach TG, Grover A, Niedzielko TL, Schneider LE, Mastroeni D, Caselli R, Kukull W, Morris JC, Hulette CM, Schmechel D, Rogers J, Stephan DA (2008) Alzheimer's disease is associated with reduced expression of energy metabolism genes in posterior cingulate neurons. *Proc Natl Acad Sci USA* 105:4441–4446
48. Blaedel WJ, Uhl JM (1975) Nature of materials in serum that interfere in the glucose oxidase-peroxidase-0-dianisidine method for glucose, and their mode of action. *Clin Chem* 21:119–124
49. Betz AL, Drewes LR, Gilboe DD (1975) Inhibition of glucose transport into brain by phlorizin, phloretin and glucose analogues. *Biochim Biophys Acta* 406:505–515
50. Wu CH, Ho YS, Tsai CY, Wang YJ, Tseng H, Wei PL, Lee CH, Liu RS, Lin SY (2009) In vitro and in vivo study of phloretin-induced apoptosis in human liver cancer cells involving inhibition of type II glucose transporter. *Int J Cancer* 124:2210–2219
51. Pedersen PL (2012) 3-Bromopyruvate (3BP) a fast acting, promising, powerful, specific, and effective "small molecule" anti-cancer agent taken from labside to bedside: introduction to a special issue. *J Bioenerg Biomembr* 44:1–6
52. Shoshan MC (2012) 3-Bromopyruvate: targets and outcomes. *J Bioenerg Biomembr* 44:7–15. Review
53. Manczak M, Park BS, Jung Y, Reddy PH (2004) Differential expression of oxidative phosphorylation genes in patients with Alzheimer's disease: implications for early mitochondrial dysfunction and oxidative damage. *Neuromolecular Med* 5:147–162
54. Reddy PH (2005) Amyloid precursor protein-mediated free radicals and oxidative damage: implications for the development and progression of Alzheimer's disease. *J Neurochem* 96:1–13. Review
55. Fujii S, Beutler E (1985) High glucose concentrations partially release hexokinase from inhibition by glucose 6-phosphate. *Proc Natl Acad Sci USA* 82:1552–1554
56. Zhu A, Romero R, Petty HR (2011) An enzymatic colorimetric assay for glucose-6-phosphate. *Anal Biochem* 419:266–270
57. Xie J, Wang BS, Yu DH, Lu Q, Ma J, Qi H, Fang C, Chen HZ (2011) Dichloroacetate shifts the metabolism from glycolysis to glucose oxidation and exhibits synergistic growth inhibition with cisplatin in HeLa cells. *Int J Oncol* 38:409–417
58. McFate T, Mohyeldin A, Lu H, Thakar J, Henriques J, Halim ND, Wu H, Schell MJ, Tsang TM, Teahan O, Zhou S, Califano JA, Jeoung NH, Harris RA, Verma A (2008) Pyruvate dehydrogenase complex activity controls metabolic and malignant phenotype in cancer cells. *J Biol Chem* 283:22700–22708
59. Kish SJ (1997) Brain energy metabolizing enzymes in Alzheimer's disease: alphaketoglutarate dehydrogenase complex and cytochrome oxidase. *Ann N Y Acad Sci* 826:218–228
60. Casley CS, Canevari L, Land JM, Clark JB, Sharpe MA (2002) Beta-amyloid inhibits integrated mitochondrial respiration and key enzyme activities. *J Neurochem* 80:91–100
61. Schwab MA, Kölker S, van den Heuvel LP, Sauer S, Wolf NI, Rating D, Hoffmann GF, Smeitink JA, Okun JG (2005) Optimized spectrophotometric assay for the completely activated pyruvate dehydrogenase complex in fibroblasts. *Clin Chem* 51:151–160

62. Patel MS, Roche TE (1990) Molecular biology and biochemistry of pyruvate dehydrogenase complexes. *FASEB J* 4:3224–3233
63. Flourmoy DS, Frey PA (1989) Inactivation of the pyruvate dehydrogenase complex of *Escherichia coli* by fluoropyruvate. *Biochemistry* 28:9594–9602
64. Galkin A, Brandt U (2005) Superoxide radical formation by pure complex I (NADH:ubiquinone oxidoreductase) from *Yarrowia lipolytica*. *J Biol Chem* 280:30129–30135
65. Cortés A, Cascante M, Cárdenas ML, Cornish-Bowden A (2001) Relationships between inhibition constants, inhibitor concentrations for 50 % inhibition and types of inhibition: new ways of analysing data. *Biochem J* 357:263–268
66. Cadenas E, Davies KJ (2000) Mitochondrial free radical generation, oxidative stress, and aging. *Free Radic Biol Med* 29:222–230
67. Pellerin L, Magistretti PJ (1994) Glutamate uptake into astrocytes stimulates aerobic glycolysis: a mechanism coupling neuronal activity to glucose utilization. *Proc Natl Acad Sci USA* 91:10625–10629
68. Krako N, Magnifico MC, Arese M, Meli G, Forte E, Lecci A, Manca A, Giuffrè A, Mastronicola D, Sarti P, Cattaneo A (2013) Characterization of mitochondrial dysfunction in the 7PA2 cell model of Alzheimer's disease. *J Alz Dis* 37:747–758
69. Calissano P, Matrone C, Amadoro G (2009) Apoptosis and in vitro Alzheimer disease neuronal models. *Commun Integra Biol* 2:163–169
70. Warburg O (1926) *Über den Stoffwechsel der Tumore*. Spring, Berlin. Translated: *The Metabolism of Tumors*. Arnold Constable, London
71. Gogvadze V, Zhivotovsky B, Orrenius S (2010) The Warburg effect and mitochondrial stability in cancer cells. *Mol Aspects Med* 31:60–74
72. Berg JM, Tymoczko JL, Stryer L (2002) *Biochemistry*. W.H. Freeman and Company, New York
73. Maher F, Davies-Hill TM, Lysko PG, Henneberry RC, Simpson IA (1991) Expression of two glucose transporters, GLUT1 and GLUT3, in cultured cerebellar neurons: evidence for neuron-specific expression of GLUT3. *Mol Cell Neurosci* 2:351–360
74. Jagus WJ, Seab JP, Huesman RH, Valk PE, Mathis CA, Reed BR, Coxson PG, Budinger TF (1991) Diminished glucose transport in Alzheimer's disease: dynamic PET studies. *J Cereb Blood Flow Metab* 11:323–330
75. Riege WH, Metter EJ (1988) Cognitive and brain imaging measures of Alzheimer's disease. *Neurobiol Aging* 9:41–42
76. Kennedy AM, Frackowiak RS, Newman SK, Bloomfield PM, Seaward J, Roques P, Lewington G, Cunningham VJ, Rossor MN (1995) Deficits in cerebral glucose metabolism demonstrated by positron emission tomography in individuals at risk of familial Alzheimer's disease. *Neurosci Lett* 186:17–20
77. Pettegrew JW, Panchalingam K, Klunk WE, McLure RJ, Muenz LR (1994) Alterations of cerebral metabolism in probable Alzheimer's disease. *Neurobiol Aging* 15:117–132
78. Reiman EM, Caselli RJ, Yun LS, Chen K, Bunduy D, Minoshima S, Thibodeau SN, Osborne D (1996) Preclinical evidence of Alzheimer's disease in persons homozygous for the epsilon 4 allele for apolipoprotein E. *New Engl J Med* 334:752–758
79. Board M, Humm S, Newsholme EA (1990) Maximum activities of key enzymes of glycolysis, glutaminolysis, pentose phosphate pathway and tricarboxylic acid cycle in normal, neoplastic and suppressed cells. *Biochem J* 265:503–509
80. Hennipman A, Smits J, van Oirschot B, van Houwelingen JC, Rijkssen G, Neyt JP, Van Unnik JA, Staal GE (1987) Glycolytic enzymes in breast cancer, benign breast disease and normal breast tissue. *Tumor Biol* 8:251–263
81. Mazurek S, Grimm H, Boschek CB, Vaupel P, Eigenbrodt E (2002) Pyruvate kinase type M2: a crossroad in the tumor metabolome. *Br J Nutr* 87:S23–S29
82. Hennipman A, van Oirschot BA, Smits J, Rijkssen G, Staal GE (1988) *Glycolytic enzyme* activities in breast cancer metastases. *Tumour Biol* 9:241–248
83. Mortilla M, Sorbi S (1990) Hexokinases in Alzheimer's disease. *Medizina (Firenze)* 10:168–169
84. Iwagoff P, Armbruster R, Enz A, Meier-Ruge W (1980) Glycolytic enzymes from human autoptic brain cortex: normal aged and demented cases. *Mech Ageing Dev* 14:203–209
85. Bigl M, Bleyl AD, Zedlick D, Arendt T, Bigl V, Eschrich K (1996) Changes of activity and isoenzyme pattern of phosphofructokinase in the brains of patients with Alzheimer's disease. *J Neurochem* 67:1164–1171
86. Pla A, Lemus L, Valenzuela A, Villanueva F (1986) Postmortem activity of the key enzymes of glycolysis. *Z Rechtsmed* 97:49–59
87. Blass JP (1997) *Cerebral metabolic impairments, Alzheimer's disease: causes, diagnosis, treatment, and care*. CRC Press, New York, pp 187–206
88. Palorini R, Votta G, Balestrieri C, Monestiroli A, Olivieri S, Vento R, Chiaradonna F (2014) Energy metabolism characterization of a novel cancer stem cell-like line 3AB-OS. *J Cell Biochem* 115:368–379
89. Macheda ML, Rogers S, Best JD (2005) Molecular and cellular regulation of glucose transporter (GLUT) proteins in cancer. *J Cell Physiol* 202:654–662
90. Xu RH, Pelicano H, Zhou Y, Carew JS, Feng L, Bhalla KN, Keating MJ, Huang P (2005) Inhibition of glycolysis in cancer cells: a novel strategy to overcome drug resistance associated with mitochondrial respiratory defect and hypoxia. *Cancer Res* 65:613–621
91. Stockwin LH, Yu SX, Borgel S, Hancock C, Wolfe TL, Phillips LR, Hollingshead MG, Newton DL (2010) Sodium dichloroacetate selectively targets cells with defects in the mitochondrial ETC. *Int J Cancer* 127:2510–2519
92. Newington JT, Rappon T, Albers S, Wong DY, Rylett RJ, Cumming RC (2012) Overexpression of pyruvate dehydrogenase kinase 1 and lactate dehydrogenase A in nerve cells confers resistance to amyloid β and other toxins by decreasing mitochondrial respiration and reactive oxygen species production. *J Biol Chem* 287:37245–37258
93. Schubert D (2005) Glucose metabolism and Alzheimer's disease. *Ageing Res Rev* 4:240–257. Review
94. Blass JP (2001) Brain metabolism and brain disease: is metabolic deficiency the proximate cause of Alzheimer dementia? *J Neurosci Res* 66:851–856
95. Minervini M, Atlante A, Gagliardi S, Ciotti MT, Marra E, Calissano P (1997) Glutamate stimulates 2-deoxyglucose uptake in rat cerebellar granule cells. *Brain Res* 768:57–62